

Modeling emergent patterns of dynamic desert ecosystems

J. STEWART,¹ A. J. PARSONS,^{2,8} J. WAINWRIGHT,³ G. S. OKIN,⁴ B. T. BESTELMEYER,⁵ E. L. FREDRICKSON,⁶
AND W. H. SCHLESINGER⁷

¹School of Engineering, University of Lincoln, Lincoln LN6 7TS United Kingdom

²Sheffield Centre for International Drylands Research, Department of Geography, University of Sheffield,
Sheffield S10 2TN United Kingdom

³Department of Geography, Durham University, Science Laboratories, South Road, Durham DH1 3LE United Kingdom

⁴Department of Geography, University of California, Los Angeles, California 90095 USA

⁵USDA-ARS, Las Cruces, New Mexico 88001 USA

⁶Department of Agriculture, Eastern Kentucky University, Richmond, Kentucky 40475 USA

⁷Cary Institute of Ecosystem Studies, Millbrook, New York 12545 USA

Abstract. In many desert ecosystems, vegetation is both patchy and dynamic: vegetated areas are interspersed with patches of bare ground, and both the positioning and the species composition of the vegetated areas exhibit change through time. These characteristics lead to the emergence of multi-scale patterns in vegetation that arise from complex relationships between plants, soils, and transport processes. Previous attempts to probe the causes of spatial complexity and predict responses of desert ecosystems tend to be limited in their focus: models of dynamics have been developed with no consideration of the inherent patchiness in the vegetation, or else models have been developed to generate patterns with no consideration of the dynamics. Here we develop a general modelling framework for the analysis of ecosystem change in deserts that is rooted in the concept of connectivity and is derived from a detailed process-based understanding. We explicitly consider spatial interactions among multiple vegetation types and multiple resources, and our model is formulated to predict responses to a variety of endogenous and exogenous disturbances. The model is implemented in the deserts of the American Southwest both to test hypotheses of the causes of the invasion of woody shrubs, and to test its ability to reproduce observed spatial differences in response to drought in the 20th century. The model's performance leads us to argue that vertical and lateral connectivity are key emergent properties of the ecosystem, which both control its behavior and provide indicators of its state. If this argument is shown to be compatible with field observations, the model presented here will provide a more certain approach toward preventing further degradation of semiarid grasslands.

Key words: patchiness; positive feedback; self-organization; semiarid landscape ecology; spatially explicit model; vegetation patterns.

INTRODUCTION

Desert ecosystems are commonly dynamic and patchy on a range of spatial and temporal scales (Ward 2008, Wainwright 2009). Their dynamism is particularly evident in long-term data showing changes in the composition and structure of plant communities (Buffington and Herbel 1965, Schlesinger et al. 1990, Archer et al. 1995, Allred 1996, Turner et al. 2003, Gibbens et al. 2005, Osborne and Beerling 2006). Their patchiness, in which vegetated areas are interspersed with areas of bare ground, varies with plant growth form. In grasslands, bare and grassy patches alternate over a few decimeters and, on sloping ground, are often associated with a stepped microtopography (Parsons et al. 1997, Dunkerley and Brown 1999, Tongway and

Ludwig 2001, Nash et al. 2004). In shrublands, the spatial scale extends to a few meters and the microtopography may comprise swales (bare patches) and vegetation atop mounds (Barbour 1969, McPherson et al. 1988, Parsons et al. 1996, Rango et al. 2000, Okin and Gillette 2001). This patchiness in vegetation can lead to the formation of striking, regular patterns such as bands of vegetation alternating with stripes of bare patches (Gillett 1941), exemplified by “tiger bush” in Africa (MacFadyen 1950, Clos-Arceduc 1956), mulga groves in Australia (Slatyer 1961), and mogote in Mexico (Cornet et al. 1988). Other geometric and irregular patterns have also been noted such as can be described as spots (Bromley et al. 1997) and labyrinths (Aguiar and Sala 1999) in the dry zones of the world.

The formation of vegetation patches has typically been explained in two ways. On the one hand, the empirical-conceptual model of islands of fertility has been used since its definition by Charley and West (1975), and especially since its development by Schlesinger et al. (1990), to explain patches at the scale of

Manuscript received 26 July 2012; revised 20 February 2013;
accepted 11 June 2013; final version received 26 October 2013.
Corresponding Editor: J. A. Jones.

⁸ Corresponding author.

E-mail: a.j.parsons@sheffield.ac.uk

individual plants. On the other hand, advection–diffusion models, usually, but not always (e.g., Lefever et al. 2009), of the Turing-instability type (e.g., Klausmeier 1999, Couteron and Lejeune 2001, HilleRisLambers et al. 2001), have been employed to explain patterns at landscape scales.

Both of the existing explanations of patchiness have shortcomings. Both have conceptual limitations, and they produce results that are mutually incompatible and difficult to evaluate independently. The islands-of-fertility approach attempts to consider the system dynamics, but it is poor at addressing the emergence of spatial patterns. Conversely, the advection–diffusion approach is able to simulate emergence of spatial patterns, but often at the expense of an appropriate characterization of the dynamics. The aim of this paper is to advance our understanding of the dynamics of desert ecosystems and the patchiness and patterns that result from these dynamics. Using a conceptual approach with an explicit process basis, a new model is developed that links the dynamics of desert ecosystems with vegetation patchiness that is both quantitative and testable against existing data.

EXISTING APPROACHES: A CRITIQUE

The islands of fertility model

The islands of fertility model (Charley and West 1975, Schlesinger et al. 1990) posits that changes in the spatial redistributions of soil resources are caused by the net transport of resources from interspaces to under-canopy areas. The heterogeneous resource distribution in turn affects plant demographic processes to reinforce vegetation patchiness. For example, during rainstorms, patches of vegetation serve as obstructions that slow, trap, and accumulate runoff, sediments, and nutrients from interpatch areas (Ludwig et al. 2005). This accumulation leads to the increase of patch biomass, which will further accumulate resources (Aguar and Sala 1999). Establishment is reported to be particularly successful around the edges of the patch where there is less competition for sunlight (Mauchamp et al. 1993), and where flows of nutrients and water become trapped, such as on the upslope edge of a patch (Montana 1992). Where individual plants die, wind- and water-induced degradation of the patch are increased, which reduces seed establishment. Propagules are then moved to other locations where they may establish new communities (Goldberg and Turner 1986).

Over time, changes in concentrations of resources may lead to new vegetation species attaining a competitive advantage within these patchy ecosystems (Osborne and Beerling 2006). For example, the widely observed encroachment of shrubs into former grasslands (Schlesinger et al. 1990, Archer et al. 1995, Allred 1996) is regarded as a process that, due to different spatial distributions of grasses and shrubs, results in self-reinforcing changes to the spatial redistributions of soil resources (Schlesinger et al. 1996). However, islands of

fertility cannot explain all the different scales at which patterns appear in desert vegetation (Müller et al. 2008). Islands have also been demonstrated to be “leaky” (Abrahams et al. 2002, Wainwright et al. 2002) and thus linked to ecogeomorphic processes occurring beyond the scale of individual islands. Furthermore, the islands of fertility model does not tell us how changes are initiated, simply why they persist. Although the model explains why invading shrubs have a competitive advantage, it does not explain how they were able to invade in the first place, nor why certain types of patterns occur (e.g., stripes) occur under some circumstances. A broader issue with the islands of fertility model is that the term itself is tautologous, and hence unsuitable for predictive purposes. If concentrations of resource are present around a shrub, it is an island. If concentrations are absent around a shrub, it is not an island. Because of the qualitative and descriptive nature of the approach (Schlesinger et al. 1990, Ludwig et al. 2005), there is nothing independent of the resource accumulations that would allow this idea to be tested. Although Schlesinger et al. (1996) used semivariograms to support the idea of spatial patterns, these patterns are still not independent of the islands that they are meant to demonstrate.

Numerical models

The use of numerical modelling to shed light on dryland vegetation has, so far, been limited in terms of its narrow focus: models of dynamics have either been developed with no consideration of the inherent patchiness or patterns in the vegetation (Thornes and Brandt 1993 [and discussion in Wainwright and Parsons 2010], Peters 2002a, Koppel and Rietkerk 2004, Istanbuluoglu and Bras 2006), or they have been developed to generate patterns with no consideration of the dynamics (Klausmeier 1999, Couteron and Lejeune 2001, HilleRisLambers et al. 2001, Rietkerk et al. 2002, van de Koppel and Rietkerk 2004, Barbier et al. 2006), or they have been parameterized to create a specific ecosystem response (e.g., Dakos et al. 2011). Furthermore, if, as seems widely believed, both dynamics, and patterns/patchiness and ecosystem responses are functions of resource (principally water) limitation, then there has been little integration into these models of the temporal and spatial variability of resource availability that are well documented for deserts (Noy-Meir 1973, Wainwright et al. 2000, Comrie and Broyles 2002).

The most prevalent type of spatial model uses a Turing-like instability to generate regular patterns in desert vegetation. Patterns (Turing structures) originate solely through the coupling of reaction and diffusion processes, and the definition of a Turing structure specifically *excludes* any type of hydrodynamic (i.e., fluid) motion (Turing 1952). Despite contravening Turing’s definition regarding applicability to hydrodynamic systems, this methodology was applied to vegetation patterns by Klausmeier (1999), whose model was based on the assumption that water cannot infiltrate

on bare areas, so it flows downhill into a vegetation stripe where it does infiltrate and support plant growth. The flow of water was assumed to be exhausted before it reaches the downslope side of the stripe where the plants will consequently die off leading to a gradual uphill movement in the vegetation bands (Montana 1992). Klausmeier's model involved the solution of two differential equations for water and plant biomass and assumed a uniform evaporation rate and water supply that is a linear function of increasing infiltration with increasing plant biomass. The model was reported to be insensitive to the exact form of functions of growth and infiltration as the resulting patterns are generated entirely by the Turing instability.

The patterns in this type of model result from spontaneous symmetry-breaking phenomena associated with bifurcations of steady states, corresponding to stable stationary solutions to a set of reaction–diffusion equations (Nicolis and Prigogine 1977, Meinhardt 1982). In Klausmeier's work, terms for water supply, infiltration, and growth represent the contributions of reactive processes while the diffusion terms, such as plant dispersal, bring in the spatial dependence. The reactive processes were set to give realistic values of the intrinsic relative periodicity of the resulting banded patterns. In doing so, however, highly implausible values for input parameters had to be set; for example, water input of up to 750 mm/yr and zero infiltration. Although some banded vegetation is found in areas with up to 750 mm/yr, this is the exceptional (of the order of two to three times higher than the rate in areas where banded vegetation is typically observed), and observed infiltration rates are non-zero (see, for example Abrahams and Parsons 1991, Casenave and Valentin 1992), requiring an even more unrealistic rainfall input to match model output.

Klausmeier's approach was extended by HilleRisLambers et al. (2001) and Rietkerk et al. (2002) so that the water input could be separated into a soil-water component. There are two major problems with the model of HilleRisLambers et al. (2001) and Rietkerk et al. (2002). First, the key conclusions drawn were that herbivory, plant dispersal, rainfall, drought intolerance, and infiltration rate are not the primary factors that are likely to form patterns in vegetation. However, these factors are represented as the reactive processes in the Turing structures. Chandrasekhar (1961) and Klausmeier (1999) had already demonstrated that only the relative periodicity of patterns depends on factors controlling the reactive processes; the resulting patterns themselves are insensitive. Model output showing the formation of patterns in vegetation that are largely not controlled by the levels of water input, plant demographic characteristics, and land-management practices is difficult to justify on the basis of our understanding of field processes. Experimental studies have identified these variables as being of significant importance (Coffin and Lauenroth 1990, Parsons et al. 1997, 2006*a, b*).

Field observations have also noted that in some areas, there is an apparent relationship between rainfall and pattern type (e.g., Deblauwe et al. 2008). However, this relationship is not universal, and very different patterns can be observed within an area of a few square kilometers, which is too small to be explained by the existence of a precipitation gradient. The second problem is that the authors reported that without positive feedback between vegetation density and water infiltration, pattern formation was not found. However, this linkage is already defined as an essential condition required for Turing instabilities, that the kinetics should include a positive feedback process (Murray 1989), so the result really states that without one of the essential conditions for Turing instabilities being included, Turing patterns do not form. Although this statement is mathematically true, it does nothing to further the understanding of pattern formation in vegetation.

These more recent models are also applicable to and capable of generating patterns on flat surfaces, and it has subsequently been argued that this result invalidates the class of model that generates patterns only when some degree of pre-patterning is first applied (Couteron and Lejeune 2001, Barbier et al. 2006). However, all reported implementations of Turing-type models require some degree of pre-patterning. For example, Rietkerk et al. (2002) perturbed small amounts of plants or water in some areas of the simulation to generate patterns, and even in the original work of Couteron and Lejeune (2001), cells in their simulation were perturbed by a low level of noise. For a Turing-type model, such pre-patterning effectively means that the model must produce a pattern. Moreover, according to Couteron and Lejeune (2001), there is no evidence in the literature of patterns appearing in arid or semiarid environments devoid of a consistent source of anisotropy.

The problems of the Turing-instability models highlight an important consideration that should be made for all numerical modelling techniques: if the underlying mathematical method is designed to generate a pattern, a pattern will be generated. This outcome is reasonable when the mathematics describe a real process. For example, following previous field observations (Thornes 1990) the model of Thornes and Brandt (1993) was set up to favor shrubs, and therefore showed a continued dominance of shrubs. By contrast, published Turing-type models of vegetation patterning do not rest on field observations, but rely on many parameters that would be difficult or impossible to measure in the field, such as “half-saturation constant,” or are defined simply to produce the desired result. Moreover, for Turing-type models, the underlying mechanism for symmetry-breaking requires coefficients to become negative under certain conditions, for example, in the formulations described here, this would mean that there could be a negative water input for certain spacings of vegetation, which is meaningless in a physical sense. This inherent lack of realism in Turing patterns was reported by

Rovinsky (1987), who noted that pattern formation could only occur where values of diffusion coefficients were in contradiction with physical arguments. Castets et al. (1990) and later Barbier et al. (2006) also observed that no unambiguous experimental observation of Turing patterns had been found. This ambiguity is drawn further into question by the contradictory conclusions drawn from Turing-instability models. For example, HilleRisLambers et al. (2001) argued that infiltration is not a primary causal factor in the formation of vegetation patterns, but van de Koppel and Rietkerk (2004) state that patterns do not form unless infiltration rate is linked to biomass. However, this linkage is not easy to define as the relationship between infiltration and biomass is not a straightforward one (Wainwright 2009).

Other fundamental problems with applications of the Turing model have been revealed when modelling results are compared to field data. The implementation reported by Couteron and Lejeune (2001) more closely follows the classic description of Turing instabilities applied to chemical reactions where the diffusion term is alternatively expressed as an activator (propagation) and an inhibitory (competition) process. In this case, the essential condition for a Turing pattern is that the inhibitor must diffuse much more quickly than the activator (Castets et al. 1990). In ecological terms, this condition would imply that the competition processes must occur over a larger scale than facilitative ones. While this difference in scale of operation may be appropriate for the consideration of a single species (e.g., a shrub canopy that facilitates growth by intercepting rainfall and channeling it to the roots operates over a smaller scale than that of competing root systems of adjacent plants [Brisson and Reynolds 1994, Martinez-Meza and Whitford 1996, Abrahams et al. 2003, Gibbens and Lenz 2005]), it is not necessarily appropriate when species of different types are competing (e.g., as shrubs invade grassland, the competition effect of canopy interception by the shrub is at the same scale as any facilitation due to shading). Furthermore, the resulting relative periodicity observed by Klausmeier (1999) was noted to be much larger than the range of interactions between plants, and it has been argued that *somehow* local processes are amplified by the spatial instability (Castets et al. 1990: 618). When the results of the model were compared to digitized images, Couteron and Lejeune (2001) found that the model yields much lower values for periodicity than were observed in field-site data. In their work, Couteron and Lejeune (2001) used realistic input data and found that the Turing model yields unrealistic intrinsic periods, whereas Klausmeier (1999) had used unrealistic input data to yield plausible intrinsic periods. A further problem arose when convincing field evidence was sought of patterns that are generated by Turing-type models, specifically the hexagonal pattern that corresponds to bare spots appearing in continuous cover of annual grasses. No

detectible hexagonal symmetry was found in the digitized images examined by Couteron and Lejeune (2001) nor in the subsequent work of Barbier et al. (2006). Many reasons were proposed to explain why this pattern could not be detected, except one—that the model had generated a pattern that does not exist in the real world because it was an inappropriate representation of the real world.

An alternative to Turing-type models is provided by other instability-based approaches characterized by representations of short-range facilitation and long-range competition (e.g., Kéfi et al. 2007, Lefever et al. 2009). While these alternative models overcome some of the limitations of the Turing-instability approach, they are nonetheless difficult to interpret in terms of physical processes.

Beyond the limitations of existing approaches

Both the islands of fertility model and those based on instability approaches address patterns in desert vegetation that exist at a specific scale (plant and patch scale). However, there has been a recognition in recent years that there are patterns in desert vegetation that exist at larger scales, such as community and landscape scales (Wainwright et al. 2002, Peters et al. 2005, Turnbull et al. 2008), which are addressed neither by the islands of fertility nor by instability-type models. The latter have been further hamstrung by the conceptual limitations of the models, applying models that are inappropriate and based on forcing process representations to fit a model structure rather than modelling the actual processes, and thus the practical limitations of producing meaningful parameterizations. Both approaches are limited by the way in which inherent problems with definition prevent adequate testing.

Modelling studies are nevertheless useful for probing the causes and consequences of the observed dynamic patterns of desert vegetation. Not only may these studies provide a rigorous test of our understanding of ecosystem functioning, they can also provide detailed information that is not readily available from experimental work (for example, due to the timescales involved in measuring changes in plant communities [Parshall et al. 2003] or due to ethical considerations such as large scale experimental modification of vegetation and landscapes). Recent conceptual advances into the understanding of multi-scale processes in drylands have focused on the role of process connectivity, drawing on broader concepts of landscape connectivity (Taylor et al. 1993, Turner et al. 1993, Western et al. 2001, Bracken and Croke 2007, Müller et al. 2007, Turnbull et al. 2008, Okin et al. 2009). Turnbull et al. (2008) suggested that spatial patterns emerge as the result of spatial feedbacks between landscape structure and process. As the structure imparted by the vegetation changes, it leads to process feedbacks, which lead to further changes in landscape structure. For example, the formation of mounds under shrubs leads to changes in

infiltration and flow pathways, which become reinforced by increased erosion rates (Parsons et al. 1996). Okin et al. (2009) provided a generic overview that suggested that connectivity across a range of processes, such as water and wind transport, animal activity, and fire, could be used to understand ongoing degradation in the U.S. Southwest. Based on this overview, it is hypothesized here that a connectivity-based model, when combined with local processes as derived from empirical work developed from the islands of fertility model, will provide a way out of the present impasse, and allow modelling studies to investigate multi-scale pattern formation in desert ecosystems. Specifically, a connectivity-based approach may provide a process-based understanding for the development of a model with advective and diffusive components that overcomes the limitations discussed above. Furthermore, if such an approach rests upon a theoretical framework with a sound process-based understanding, it can thus be parameterized with data that can be measured and have a clear physical meaning. Testing the ability of such a model to reproduce the spatial and temporal progression of vegetation patterns, will enable it to be used with confidence to generate testable predictions relating to the function of dynamic desert ecosystems in response to a variety of endogenous and exogenous disturbances.

MODELLING FRAMEWORK

The ecogeomorphic modelling framework proposed here (Fig. 1) meets the characteristics outlined above. In this framework, the environment is represented as spatially related locations that may be inhabited by different vegetation types and quantities. Processes operating within the landscape are considered as being either vertical or lateral. Vertical processes act as inputs (e.g., rainfall or atmospheric deposition of nitrogen) or outputs (e.g., losses of biomass through herbivory), while lateral processes act entirely within the system (e.g., movement of propagules by water). These processes provide locations with resources and propagules (R and P) that are the main drivers of plant growth and recruitment. Resources are defined in the model as abiotic materials that plants need to grow and propagate. Although the model can include any number of resources, emphasis has been placed on water and nitrogen as the principal limitations on growth in deserts (Fitter and Hay 1987, Whitford 2002:14, Wainwright 2009). Propagules are biotic materials required for reproduction (e.g., seeds, tillers, cladodes).

The lateral processes controlling the movement of R and P can be expressed as a set of vectors. Three vectors are included in the model: water, wind, and animals. However, in principle, any number could be included. The ability of vectors (in the sense of a geometric entity, having both a direction and magnitude) to redistribute R and P within the landscape is controlled by external factors. These external factors are termed “lateral externalities.” For instance, the movement of propagules

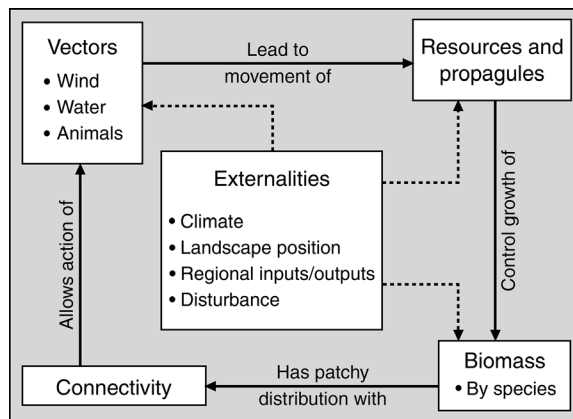


FIG. 1. Conceptual framework for modeling dynamic relationships between elements of desert ecosystems. The modeled processes are denoted by the solid arrows, and the externalities that influence those processes are denoted by the dashed arrows.

by wind depends on wind speed and direction (Okin et al. 2001). The movement of material by water depends on raindrop energy, the infiltration-excess runoff, surface topography and the characteristics of the material being moved (Parsons et al. 2004). Animals move material according to foraging strategies. For instance, large grazing mammals can move large amounts of organic carbon and nitrogen in their guts over great distances, while propagules can be moved internally or externally as burrs and cladodes attached to the hide of the animal (Turchin 2003).

Similarly, the vertical processes that move R and P into and out of the landscape are controlled by external factors, termed “vertical externalities,” which include infiltration, leaching, evaporation and wet/dry deposition of nutrients or seeds. Direct disturbance of biomass is controlled by disturbance factors, termed “disturbance externalities,” which include destruction or removal of biomass by fire, disease, or herbivory.

The operation of the vectors that control the movement of R and P can be subdivided into two broad process states. These two process states are advection and diffusion. The important advective processes are concentrated overland flow (Wainwright et al. 2008a), aeolian transport through large interplant gaps and the movement of, typically, large animals through the landscape. They are a function of lateral externalities such as wind strength, flow hydraulics, or the type and number of large animals. The important diffusive processes are splash, local distribution by small eddies and movements caused by small animals.

For the purpose of the model, connectivity quantifies the extent to which individual cells of the landscape may receive a subsidy as a result of the operation of a specific vector. The effectiveness of vectors to move R and P in the direction of flow depends on the spatial arrangement of what are termed connected pathways (Bartley et al.

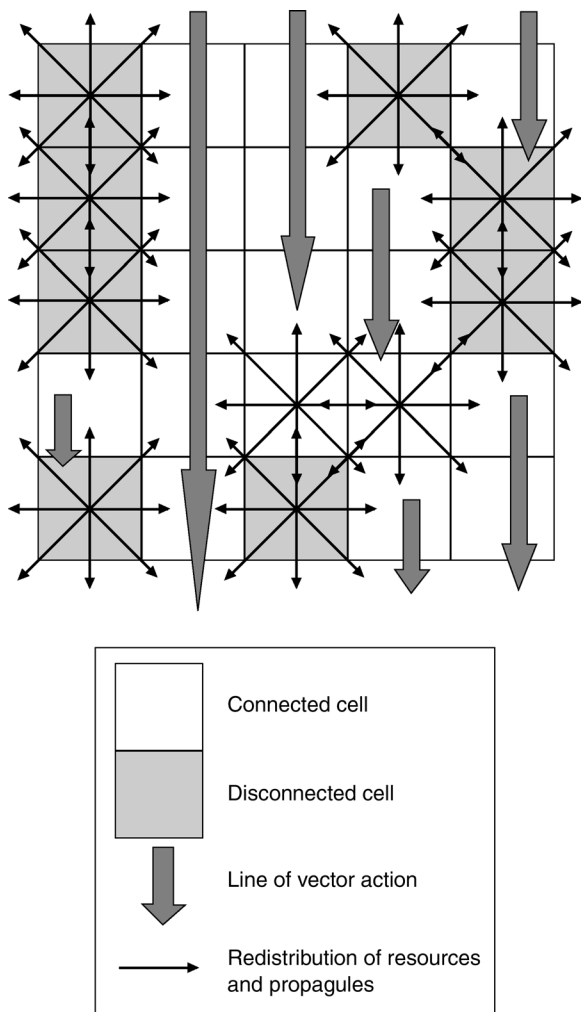


FIG. 2. The mechanisms for resource and propagule redistribution based on cell connectivity. If a cell is disconnected (i.e., receives no input of resources and propagules from up-vector cells), or is at the end of a connected pathway, available resources and propagules entering that cell are redistributed according to rules given in Table 3. If the cell lies on a connected pathway, available resources and propagules are moved down-vector.

2006). For wind, connected pathways are quasi-linear, aligned with the direction of the wind, and terminated when wind intersects a plant (Okin and Gillette 2001, Okin et al. 2009). For water, gross pathways follow the energy slope and net pathways follow the aspect. For animals, the definition of connected pathways depends on the behavior of individual species, for example, for large grazing mammals; a connected pathway is defined as contiguous areas with palatable biomass above a threshold amount (Turchin 2003, Thornes 2007). In the model, all connected pathways terminate in sinks. For example, a shrub would terminate the wind vector, a vegetation patch would terminate the water vector, and an unvegetated area would terminate the grazing vector. A diagrammatic representation of connected pathways

and their terminations is shown in Fig. 2. The behavior of the biomass controls the number and arrangement of connected pathways. However, because connectivity is also an emergent property of the model, reflecting the feedbacks between the vectors and vegetation growth and death, it is also an independent measure of the ability of the model to represent the dynamics of desert ecosystems: if the processes in the model operate in a way that is compatible with reality, then connected pathways should be observable in real landscapes, and rates of change should also be equivalent.

Not all distributions of R and P are amenable for movement by vectors. Labile nitrogen beneath canopies, for instance, cannot be moved by infiltration-excess runoff occurring in plant interspaces. The extent to which R and P are amenable to movement by vectors is specified in the model as "availability." Availability is controlled by the biomass content in each spatial location. For wind and water, which cannot (under non-drought conditions) remove material from under-canopy areas, R and P may only be removed from plant interspaces. Animals, in turn, can forage only where there is a significant amount of palatable forage.

Demographic processes (recruitment, establishment, growth, and mortality) control the amount of biomass of individual species (e.g., Coffin and Lauenroth 1990). The spatial patterning of structurally diverse vegetation controls the strength of vectors acting on the land surface (e.g., Okin and Gillette 2001). For example an open plant community would allow for a greater number of connected pathways along which wind and water could operate, but some species of plants do not provide palatable forage and so reduce the number of grazer-connected pathways. The latter reduction in connectivity in turn affects the redistribution of R and P , resulting in sinks of resource where plants are more likely to become established and survive. Therefore, this model explicitly considers relationships among the forces that control R and P movement via vertical and lateral externalities and vegetation distribution via connectivity. As a first approximation, it is assumed that soil mechanical properties (including density and hardness) may be neglected and so plant growth is assumed to be equally possible in all locations (Bugmann and Solomon 1995, Higgins et al. 1996, Starfield 1996), though, as with the number of vectors, such variables could, in principle, be incorporated into the model.

NUMERICAL IMPLEMENTATION OF THE MODEL

In order to represent the spatial arrangement and structure of the simulated ecosystem, the area under consideration is divided into a grid of equally spaced nodal points enclosed by square cells of equal size. The number of cells used is specific to the particular implementation. The placement of these points coincides with the physical boundaries of the grid. A general point L and its neighbors are identified using a Moore

neighborhood of the eight neighboring points (Fig. 3). In order to limit the effects of numerical boundary conditions, cells are always wrapped (i.e., to form a cylinder) in the direction perpendicular to the vectors using a simple up-and-down procedure (Furukawa et al. 2000). For water, the direction of the vector is defined (arbitrarily and in this implementation of the model) as north to south, implying a sink of water at the southern edge of the grid. Therefore, the line of action for grazers is south to north (that is, away from the implied water source, e.g., Lange et al. [1984]). For both water and grazers, cells are consequently wrapped across the east and west boundaries. Wind is allowed to operate in any direction across the grid, but in the present implementation, the line of action is east to west so the north and south boundaries are wrapped. A periodic boundary condition is applied in the direction aligned with the vector (Leach 2001) when the grid represents a terrain with no slope. This condition was also applied to the application of the model described below to demonstrate that numerical boundary conditions did not affect the model results.

The model operates with an annual time step. For each cell, the change in resource and propagules (represented through the term Z) in each time step (t) is as a result of three actions. These are the actions of vertical processes (Q_v), which add or remove material to the cell, the lateral processes (Q_H), which redistribute material in the grid, and the action of plant species (U), which varies depending on whether resources or propagules are being considered: where abiotic resources are considered, U represents a consumption term and, where propagules are considered, U represents a production term. The change in each i abiotic resource and biotic propagule for each cell can be expressed in differential form

$$\frac{dZ_i}{dt} = \frac{dQ_{v_i}}{dt} + \frac{dQ_{H_i}}{dt} + \frac{dU_i}{dt}. \tag{1}$$

The model needs to be general enough to allow a range of physical processes to operate within the grid. However, different physical processes will operate over different spatial and temporal scales. The different spatial scales are accounted for by parameterizing the model according to the size of the cells used in the implementation, but a different procedure must be used for defining the various temporal scales. For example, a summer monsoon-type rainstorm will quickly lead to the generation of overland flow (Parsons et al. 1997), whereas processes allowing this water to infiltrate, particularly to deeper soil layers, may take considerably longer (Hillel 2004, Wainwright 2009, Wainwright and Bracken 2011). In order to calculate the physical responses of such a system, Peters (2002a) used daily totals (for example rainfall rate), which were summed to monthly totals, whereas the more appropriate yearly values for biomass were aggregated over each month. Eq. 2 is therefore cast to reflect different temporal scales

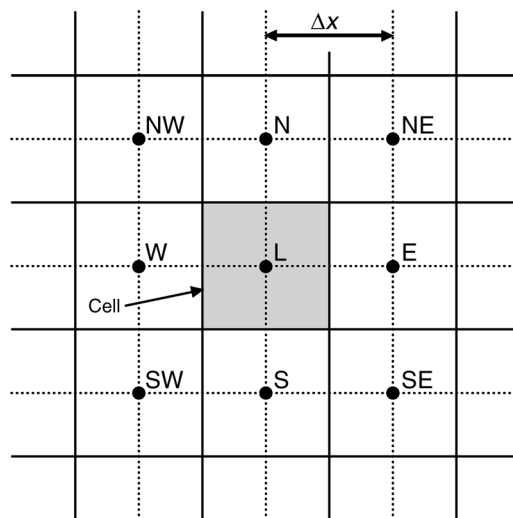


FIG. 3. Simulation grid showing an arbitrary cell and its Moore neighborhood. Labeling of the neighbors denotes their direction with respect to the grid; Δx denotes cell size.

(represented by θ , ϕ , and ψ) summing to the same time scale (t)

$$Z_i = \int_t^{t+1} \left[\left(\frac{dQ_{v_i}}{d\theta} \right) \frac{d\theta}{dt} + \left(\frac{dQ_{H_i}}{d\phi} \right) \frac{d\phi}{dt} + \left(\frac{dU_i}{d\psi} \right) \frac{d\psi}{dt} \right]. \tag{2}$$

The different timescales imply that different processes are applied in a strict order (from fastest to slowest) in the calculation, and each process is enclosed within its own iterative loop. The numerical solution is therefore formulated so that the first calculation procedure adds or removes R and P by vertical processes. Subsequently, the R and P are redistributed by lateral processes. Finally the biomass is allowed to respond to these new R and P distributions at the end of the time step (Fig. 4). All results presented below are for the aggregated effects of these timescales at an annual resolution.

Vertical processes

Vertical processes are those that can move R and P into and out of the landscape without intermediate movement across the surface of the grid. To represent different processes, the Q_v term is divided into two parts. The first part (Q_{v_ex}) represents those processes controlled wholly by vertical externalities, and thus operate independently of the biomass in the cell (e.g., precipitation rates); the second part (Q_{v_in}) comprises those vertical processes linked to cell biomass (e.g., infiltration rates [internal]). For simplicity of implementation, the effects of disturbance externalities are also included within vertical processes and can be internal or external according to whichever disturbance externality is being considered. The term Q_v is therefore a representation of the output of suitable sub-models to describe these phenomena

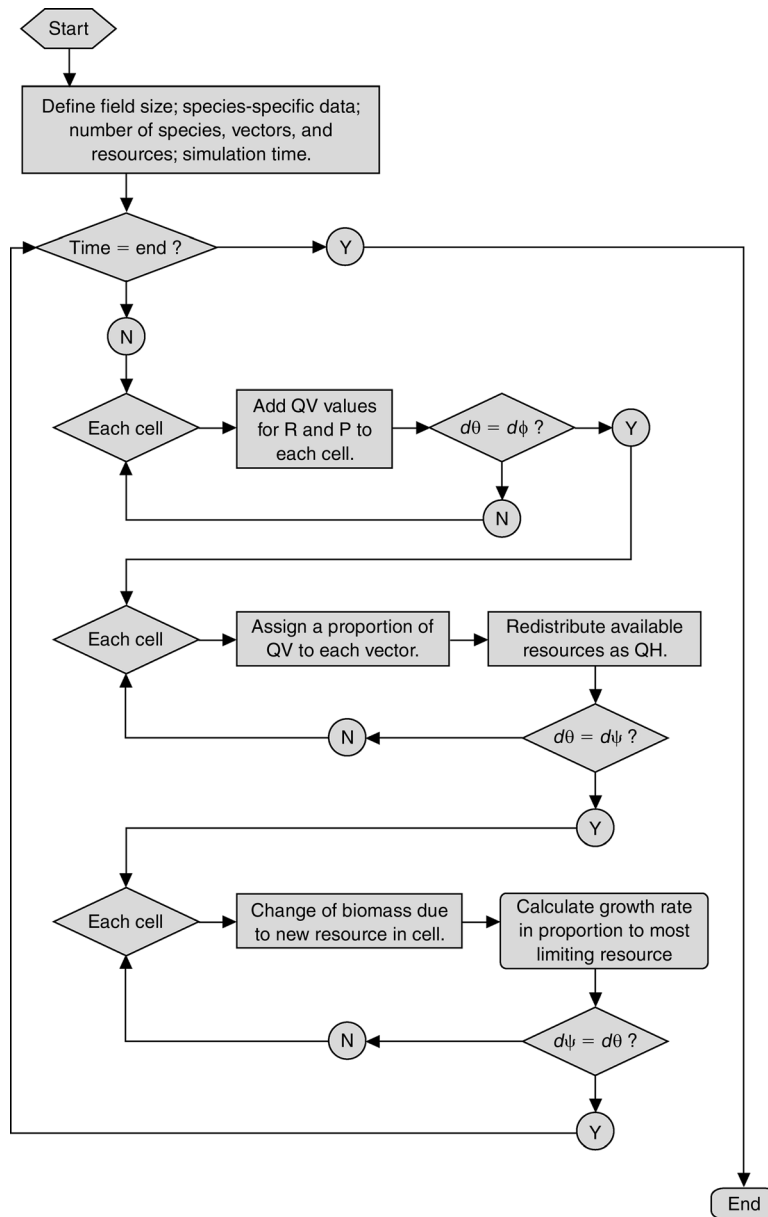


FIG. 4. Schematic diagram of model execution in which QV is input from vertical processes; QH is redistribution by lateral processes; R is resources; P is propagules; and θ , ϕ , and ψ are three temporal scales. N stands for “no” and Y stands for “yes.”

$$Q_{V,i} = Q_{V,i,ex} + Q_{V,i,in}. \quad (3)$$

By defining a spatial grid of nodal points, the model has the flexibility to include appropriate sub-models for spatial variability that apply to the process in question.

Lateral processes

The extent to which R and P are amenable for movement by vectors, is specified by the “availability” (A) term, which is itself a function of biomass in each spatial location. We define a maximum biomass (B_{max}) for each species that can exist in each cell and a linearly decreasing amount of R and P (Greene et al. 1994,

Morgan 1996) is available to the water and wind vectors as the actual biomass in the cell increases as

$$A_{i,cell} = \left[Z_i - Z_i \frac{B}{B_{max}} \right]_{cell} + Q_{up,i} \quad (4)$$

while a linearly increasing amount of R and P is available to grazers as biomass increases

$$A_{i,cell} = \left[Z_i \frac{B}{B_{max}} \right]_{cell} + Q_{up,i}. \quad (5)$$

For all three vectors, the availability of propagules increases with biomass (Eqs. 4 and 5). The availability

term also includes the R and P moved into the cell from its up-vector neighbor ($Q_{up,i}$).

When the connected pathways are terminated, the sum of the resource that has been entrained by the vector along the connected pathway is redistributed from the cell terminating the connected pathway, i.e., R and P movement becomes a diffusive, internally controlled process. The form of this redistribution is modelled by a series of convolution matrices that are specific to each transport vector and each sink (e.g., shrub or grass). It is assumed that, upon encountering a cell terminating a connected pathway, and in all subsequent vegetated cells along the line of action of the vector, some proportion of the entrained R and P ($\alpha, \beta, \gamma, \epsilon,$ and ζ according to the relative position; see Eq. 6) is redistributed to the eight cells that surround the disconnected cell. First, the R and P move down-flux is combined with the available R and P of the current cell into a single term, Q_{ADV} , (the sum of all the available R and P). It is considered that part of this R and P remains in the current cell, lateral distributions of R and P from the current cell are symmetrical, but redistributions along the line of the vector can be asymmetrical. These descriptions are summarized in Eq. 6, using the water vector as an example. Except for the R and P that is advected to the south cell, the R and P that is redistributed to the neighbor cells is unavailable for further movement by the vectors in the current time step. For the other vectors, the equation set is rotated relative to the appropriate direction of operation of the vector (northwest, NW; north, N; northeast, NE; west, W; current cell, L; east, E; southwest, SW; south, S; and southeast, SE)

$$\begin{matrix}
 \text{NW, } \frac{\epsilon}{2} Q_{ADV} & \text{N, } \beta Q_{ADV} & \text{NE, } \frac{\epsilon}{2} Q_{ADV} \\
 \text{W, } \frac{\alpha}{2} Q_{ADV} & \text{L, } Q_{ADV}(1 - \alpha - \beta - \gamma - \epsilon - \zeta) & \text{E, } \frac{\alpha}{2} Q_{ADV} \\
 \text{SW, } \frac{\zeta}{2} Q_{ADV} & \text{S, } \gamma Q_{ADV} & \text{SE, } \frac{\zeta}{2} Q_{ADV}
 \end{matrix} \quad (6)$$

This description links the amount of R and P that is moved to the magnitude of the external controls, in the sense that larger rainfall amounts result in a greater amount of R and P moved via the lateral processes compared with drought years. It should be noted that the length and spatial arrangement of the connected pathways depends upon biomass response, which itself is a function of lateral and vertical processes that occurred during previous time steps.

Only the R and P that is added in the current time step is moved in this way. Propagules are either established as seedlings or fail to establish before subsequent calculation steps, and any resource remaining from previous time steps is considered as unavailable to the lateral processes and moved down through the soil layers by the vertical processes. All resource, whether

added and moved in the current time step or accumulated from previous time steps is then available to be used by the biomass for growth and propagation.

The derivation of the convolution matrices is analogous to the discretization of partial differential equations to describe the diffusion of R and P around the current cell, and is based on the finite volume method for computational fluid dynamics (e.g., Versteeg and Malalasekera 1995). As such, this model can be implemented (via Eq. 6) analytically, where explicit equations control spatiotemporal dynamics, or numerically, where dynamics are controlled by a combination of analytical equations and neighborhood-based rules. In the present implementation, these convolution matrices are specified as neighborhood-based rules that encapsulate the detailed biophysical processes that result in the deposition, and patterns of deposition, of material in the vicinity of plants. This neighborhood-rule approach allows the transport of material by vectors to be included explicitly without the computational burden of having to model the sub-grid-scale physics explicitly.

Biomass response

Any suitable model for vegetation-growth dynamics can be included through the term U (in Eqs. 1 and 2). The present implementation of the model is designed to test the extent to which local redistribution of R and P can lead to emergent patterns of desert vegetation, and so to include a logistic growth equation here (e.g., Thornes and Brandt 1993) would mask the effects of changing R and P when the biomass content of a cell is near to zero or the carrying capacity (Kot 2001). Biomass is thus allowed to change linearly in response to new resource levels in the cell.

The change in biomass (ΔB_j) for each species j is calculated using the sum of each resource in the cell ($R_{tot,i}$), which includes the redistributed resource from the current time step plus any resource remaining from previous time steps, which is stored in the lower soil layers. The actual change in biomass is computed from the most limiting of the resources

$$\Delta B_{j,i} = \left[\frac{R_{tot,i} - B_j M_{i,j}}{E_{i,j}} \right] \quad (7)$$

M is the required amount of each i resource to maintain 1 g of perennial material in the plant (used here to describe the resource requirement for maintenance of biomass) and E is the resource needed to yield 1 g of new leafy material (used here to describe the resource requirement for new growth; Peters 2002a). This method allows the model to describe vegetation response by process, as multiple species may be parameterized using data that can be measured in the field. As such, multiple actual species are represented, unlike the majority of previous spatial modelling work where generic grass- or shrub-type species have been considered as broad functional types (Thornes and Brandt 1993, Klausmeier

1999, Couteron and Lejeune 2001, HilleRisLambers et al. 2001, Rietkirk et al. 2002, Koppel and Rietkerk 2004, Barbier et al. 2006, Istanbuluoglu and Bras 2006).

MODEL IMPLEMENTATION

In order to test the numerical model, it has been implemented with respect to parameters and conditions in the deserts of the southwestern United States. Two sets of simulations have been conducted, but only the latter are presented here. In the first, a series of simulations was carried out to explore the behavior of the model. These simulations are reported in the Appendix. They showed agreement of the behavior of our model with observed characteristics of desert vegetation, giving us confidence to use the model test hypotheses of vegetation change in the American Southwest.

The American Southwest is one of the many regions in the world where invasion of woody shrubs into desert grassland has been observed (Schlesinger et al. 1990, Archer et al. 1995, Allred 1996). Increasing aridity (e.g., Archer et al. 1995, d'Herbes et al. 2001) and overgrazing (e.g., Westoby et al. 1989, Archer et al. 1995, Gibbens and Lenz 2001, Okin et al. 2001, Nash et al. 2004) are commonly used explanations for shrub invasions into grasslands. Thus, here we use the model to investigate the viability of these explanations both individually and in combination, and to propose testable hypotheses of why changes in desert ecosystems are initiated. A further advantage of the use of this region for an implementation of the model is that it is relatively data rich, and thus some information exists that can be used to provide an independent test of the model output.

The specific site chosen for model implementation is the Jornada Basin Long Term Ecological Research site in southern New Mexico (32°37' N, 106°40' W, 1260 m above sea level). The Jornada Basin LTER was established with the task of quantifying the processes that have caused dramatic changes of structure and functioning of Chihuahuan desert ecosystems, such as have been noted over the past 150 years, and links into preexisting and continuing datasets collected by the USDA-ARS Jornada Experimental Range field station. An impressive array of data is available for the Jornada Basin, which makes it possible to look for temporal trends, spatial patterns and ecosystem changes over the 20th century (Wainwright 2005, Havstad et al. 2006, Yao et al. 2006). Consequently, the region, and particularly the LTER site, is rich in data with which to parameterize our model. The Jornada Basin LTER experiences severe drought (Palmer Drought index between -3 and -4 [Nicholson 1979, 1981]) every 20–25 years, and extreme drought (Palmer Drought index of <-4) occurs every 50–60 years. Livestock were introduced from Mexico during the early part of the 16th century, but grazing was limited in the Jornada Basin owing to the lack of surface water until the sinking of the first wells in 1867 following the Homestead Act of

1862. Since then, it has supported a mainly beef rangeland livestock industry (Gibbens et al. 2005, Havstad et al. 2006). For many arid and semiarid ecosystems the amount of biomass supported per unit area of primary production is approximately an order of magnitude greater under rangeland livestock production than under natural non-agricultural conditions. For example, in the Jornada the biomass of native consumers is approximately 0.03 g/m^2 , which consume less than 5 g/m^2 of forage per year compared to a conservative stocking rate of cattle of 1.7 g/m^2 , which consume $8\text{--}14 \text{ g/m}^2$ per year on the same grassland (Havstad et al. 2006; but see also Pieper et al. 1983).

Model parameterization

A realistic test of the conceptual model should be undertaken with reference to specific localities and specific species if insights beyond broad generalizations are to be gained. Such site-specific insights are a prerequisite for informed management interventions (Westoby 1980). Accordingly, parameterization is based, as far as possible on data obtained from field measurements at the Jornada LTER, or elsewhere in the U.S. Southwest. For the implementation, we use a planar $50 \times 50 \text{ m}$ grid that is subdivided into cells of 1 m^2 with a downslope gradient of 2° north-south. A summary of the model input conditions is presented in Table 1.

Biomass.—The encroachment of grassland by woody shrubs may involve several species, but in this implementation of our model, plant demographic processes were parameterized using two species that are indicative of the grass to shrubland transitions observed in the deserts of the southwestern United States (Humphrey and Mehrhoff 1958, Schlesinger et al. 1990, Peters 2002a, b). These two species are *Bouteloua eriopoda* (Torr.) Torr. (black grama) and *Larrea tridentata* (DC.) Coville (creosotebush). The first represents a typical desert grass, which is the dominant species in many hot desert grasslands of the southwest United States (Nelson 1934, Smith et al. 1996). Black grama typically occurs on rocky or sandy mesas and open ground, with well drained sandy and gravelly soils (Humphrey 1958) and is particularly abundant in the Chihuahuan desert (Peters 2002b, Yao et al. 2006).

Black grama often shows an association in upland areas with our second simulated species, creosotebush (Gardener 1950). Creosotebush is a drought-tolerant, evergreen shrub and a dominant or co-dominant member of many plant communities in the Southwestern deserts (Humphrey 1958). It usually occurs in open, sparsely populated areas, but also appears as a transitional species in desert grasslands (Humphrey and Mehrhoff 1958), and is noted to grow on bajadas, gentle slopes, valley floors, sand dunes, and in arroyos, typically on calcareous, sandy, and alluvial soils that are often underlain by a caliche hardpan (Went and Westergaard 1949). Creosotebush occurs as far south

TABLE 1. Summary of input conditions used in model simulations.

Parameter	Input condition
Length of rainfall record used in simulations	312 yr, 80 yr, or 80-yr average
Size of grid	50 × 50 m
Gradient of slope	2°
Nitrogen input	0.65 g/m ²
Water input to each cell	constant, long-term average = 228 mm/yr; stochastic, average = 243 mm/yr; measured, average = 243 mm/yr

as north-central Mexico, and as far north as central Nevada (Ackerman and Bamberg 1974, Pockman and Sperry 1997), where average annual rainfall ranges from 100 to 300 mm (Castellanos and Molina 1990).

Externalities and vertical processes.—The instrumental record for rainfall at the Jornada begins in 1914, so longer term data for rainfall are only available by reconstructions. Tree-ring data have been used to reconstruct climate data in the US Southwest for the time period extending over the last few hundred years (d'Arigo and Jacoby 1992), that includes the period of introduced cattle grazing. Data are available from the International Tree Ring Databank for three locations within a 50-km radius of the Jornada Basin, which were used by Wainwright (2005) to reconstruct a common sequence of the Jornada climate (Fig. 5a) extending from 1659 to 1970. Comparison with the more recent instrumental record (approximately 80 years long) suggests that although the retrodictions can capture extreme events, they tend to underestimate the magnitudes of these events (Fig. 5b). Cycles were present similar to those in the instrumental record, and drought conditions were retrodicted for the years 1676, 1790, 1721, 1723, 1736, 1872, and 1912. Greater interannual variability (in terms of number of rain days, rainfall totals, and annual moisture balance) were noted until the late 18th century, whereas the 20th century seems to be particularly anomalous with long wet periods alternating with dry spells. The reconstructed rainfall record provides a regional input in terms of precipitation to our model, and includes disturbances due to drought implicitly.

Cattle-stocking levels over the 20th century for which historical data are available (Havstad et al. 2006) are shown in Fig. 6. Disturbance due to grazers is modelled explicitly by simulating the removal of a specified quantity of palatable biomass from each vegetated cell, in each year. A summary of the simulated grazing levels is presented in Table 2, which reports the minimum and maximum of harvest rates for cattle under three different stocking levels described as conservative, recommended, and overgrazed by Havstad et al. (2006). In our simulations, we used the central value of the reported consumption range.

Lateral processes.—In this implementation, three vectors are defined: water, wind, and animals. As the action of grazers is being modelled as a disturbance

externality, the animal vector in this implementation represents the action of cattle. The model requires rules for the proportion of resources and propagules that can be moved by each vector, and, although all the parameters used in this model could be measured at the field site, as yet much of this information is not available in a form that can be implemented numerically. Consequently, we have inferred the R and P availability and convolution matrices from experimental work that alludes to the mechanisms by which vectors might operate (Parsons et al. 1992, 1997, 2004, 2006a, b, Okin and Gillette 2001, Okin et al. 2001, 2009), and also from process-based modelling studies (Scoging et al. 1992, Parsons et al. 1997, Wainwright et al. 1999, 2002, 2008a–c). We specify that, of the resource added to each cell per time step by the vertical processes, water cannot be moved from cell to cell under the action of wind or grazers, and we allocate 45% of the nitrogen to be amenable to movement by water, 45% to be amenable to movement by wind, and 10% to be amenable to movement by grazers. These proportions are arbitrary, but based upon the argument that wind and water have equal access to nitrogen in the soil, whereas grazers have access only via vegetation uptake. The redistribution of R and P from vegetated cells is effected according to the species-specific rules defined in Table 3 for water-disconnected locations, wind-disconnected locations, and grazer-disconnected locations.

Resources and propagules.—Aside from rainfall and grazing externalities, model parameterization requires information about the abiotic resources necessary to support plant activities. Although the model can be parameterized to accommodate any number of resources, we have focused on two in this implementation: water and nitrogen. The water input to the model is provided through the descriptions of rainfall described previously.

It is, however, difficult to find suitable parameterization data for nitrogen. The analysis of the plant-available nitrogen in the soil is not a particularly useful measure of the total nitrogen available to plants, since nitrogen released by microbes can be rapidly taken up by plants and never appear in the soil pool (Gallardo and Schlesinger 1992). This issue is noted to be particularly important in semiarid environments (Clark and Tilman 2008). The point at which nitrogen becomes limiting to plant growth at the Jornada, under condi-

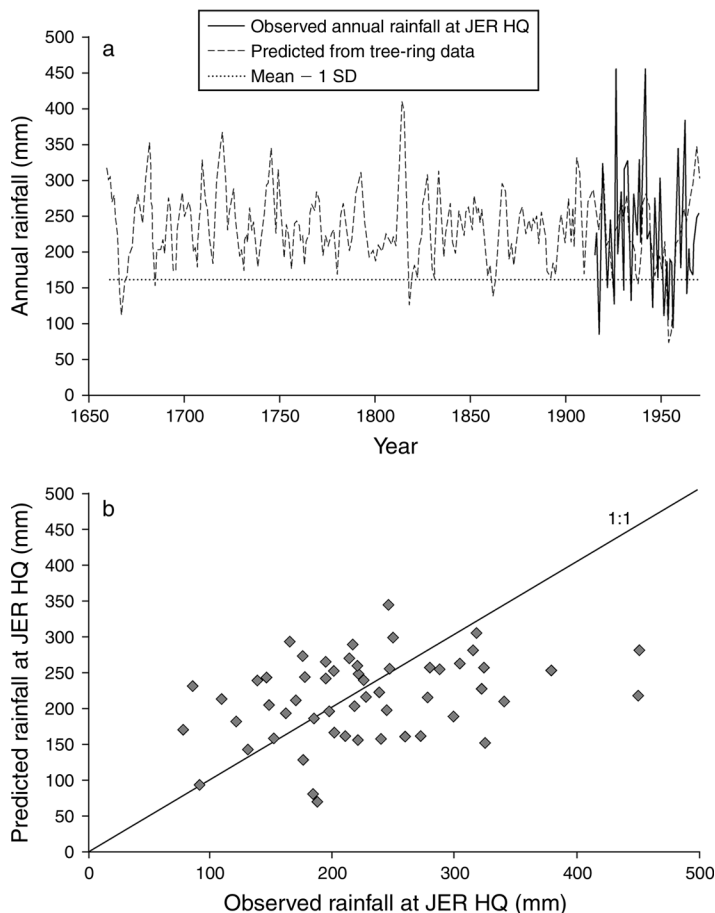


FIG. 5. (a) Rainfall data reconstructed from tree-ring data at the Jornada headquarters (JER HQ) from 1659 to 1969. Measured values from the instrumental record are plotted from 1915 to 1995 for comparison (Wainwright 2005). Assume water has a density of 1 Mg/m^3 , so g/m^2 are equivalent to mm. (b) Comparison of reconstructed with real rainfall data over common years at the Jornada headquarters (Wainwright 2005). Root mean square (RMS) is 82.5 mm and normalized root mean square error (NRMSE) is 36.5%.

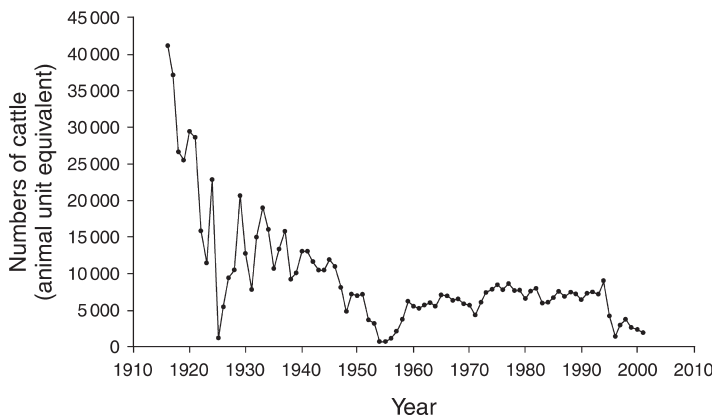
tions when water is not limiting, must be answered in the short term, as a longer-term perspective would allow the invasion of non-desert vegetation, with much higher productivity, assuming that such vegetation possesses the necessary adaptations to semiarid environments. In the short term, it seems that nitrogen is limiting whenever water (the dominant control in its own right and through its partial control on nitrogen availability) is non-limiting, so the present rate of nitrogen mineralization of up to $5 \text{ g}\cdot\text{m}^{-2}\cdot\text{yr}^{-1}$ (Loreau et al. 2002) would be the lower limit to plant growth in various habitats. The rate of annual nitrogen mineralization has not been measured in much detail since many researchers believe periods of rapid mineralization probably occur during a few wet months, and then no mineralization takes place for the rest of the year. Thus, nitrogen inputs were simulated as a constant values in this work (Baez et al. 2007), but the amount of nitrogen that is used by the plants to support existing biomass and, for new growth, was allowed to vary linearly with rainfall (Burke et al. 1990, Peters 2006a, Wainwright 2009).

After a resource has been added by vertical processes, and moved by the lateral processes, it is then used to support plant growth. Descriptions of resource use by

the biomass (Table 4) are based on data given in Peters (2002a), Maneta et al. (2008), and Wainwright (2009).

The consumption of resource by the biomass is calculated using the sum of each resource in the cell, which includes the resource from the current time step plus any resource remaining from previous time steps, which are stored in the middle and deep soil layers. Three soil layers are simulated. The top layer, from depths of 0 to 100 mm, contains resource added in the current time step, and subsequently redistributed by the vectors. The depth was selected to coincide with measured wetting-front depths (Martinez-Meza and Whitford 1996, Parsons et al. 1997, Wainwright et al. 2008b, c). The middle layer, from depths of 100 to 350 mm, corresponds to the maximum observed depth for root-channelized water in creosotebush (Martinez-Meza and Whitford 1996, Scott et al. 2008) and encloses the point of maximum root density for both creosotebush and black grama (Martinez-Meza and Whitford 1996, Sun et al. 1998, Gibbens and Lenz 2001, Peters 2002a). The deep layer, from depths of 350 to 1500 mm, corresponds to the maximum observed depth of creosotebush roots (Gibbens and Lenz 2001, Peters 2002a).

FIG. 6. Stocking levels of cattle (represented by animal unit equivalents) in the Jornada basin from 1915 to 2001. An animal unit is a mature, non-lactating 1100-pound (498.95 kg) beef cow consuming 26 pounds (11.793 kg) of forage per day.



Black grama is an intensive exploiter of water and derives the majority of its moisture through dense root networks in shallow soil layers that enable it to exhibit rapid growth and water absorption following rainfall. Black grama tolerates short droughts, and recovers rapidly from stress when water is available (Burgess 1995). These factors are reflected in the higher proportion of roots in our simulated top layer, which allows grass to access the resources that are added in each time step ahead of creosotebush. During conditions with adequate water input, the top and middle layers will receive a greater quantity of water, and this will favor the grass (Walter 1971, Thornes 1990). Creosotebush has a greater proportion of roots in the middle and particularly the deep layers where unused resource from previous time steps is stored. During times of resource stress, creosotebush can access this store ahead of black grama, reflecting the greater drought tolerance of shrubs (Walter 1971, Herbel et al. 1972, Casper and Jackson 1997). These arguments represent competition processes between the species (Thornes 1990).

The proportion of resource in each layer that can be used by each species is a function of root biomass (Table 5, Fig. 7). The aboveground biomass is converted to belowground biomass using the relationship proposed by Peters (2002a), wherein black grama root biomass is estimated to be 1.44 times greater than the aboveground biomass, and the root biomass of creosotebush is estimated to be equal to the aboveground biomass. In order to distribute root biomass among the layers, we follow the method described by Peters (2002a), which was itself based on the analyses of root distributions of a

large number of grassland species in the United States by Sun et al. (1998). The method assumes that root biomass increases linearly to a species-specific depth, then decreases allometrically to the maximum depth. Parameterization data were all obtained from Peters (2002a).

If creosotebush is the dominant species in the cell, then a proportion of the top-layer resource (equal to the proportion of creosotebush biomass in the cell) is directly channeled into the middle and deep layers (Martinez-Meza and Whitford 1996, Abrahams et al. 2003). The movement of resource through the soil layers acts as a facilitation term. Once established, creosotebush is thought to improve sites for the annual plants that grow beneath its canopy by trapping sediment, organic matter, and propagules, and by increasing water infiltration and storage (Bainbridge and Virginia 1990). Although this description of channelization should strictly apply only to water, nitrogen is also handled in the same way in the model implementation to reflect the ability of a plant with access to deep water to use more of other nutrients (Martinez-Meza and Whitford 1996), and it is reasonable to assume that the water contains significant amounts of dissolved nitrogen (Schlesinger et al. 1990, Schlesinger and Peterjohn 1991, Grimm and Railsback 2005, Brazier et al. 2007, Turnbull et al. 2010, Michaelides et al. 2012).

In each cell, if there is insufficient resource at a particular time step to satisfy maintenance requirements, the biomass is reduced. When the outcome is a loss of biomass, and this loss is due to insufficient water, the model allows all water to be used but no other resources

TABLE 2. Ranges of biomass consumption under three different grazing strategies (Havstad et al. 2006).

Range	Conservative		Recommended		Overstocked	
	Amount consumed (g·m ⁻² ·yr ⁻¹)	Percentage consumed (%)	Amount consumed (g·m ⁻² ·yr ⁻¹)	Percentage consumed (%)	Amount consumed (g·m ⁻² ·yr ⁻¹)	Percentage consumed (%)
Lowest quoted value	8	2.5	7	2.2	30	9.4
Highest quoted value	14	4.4	21	6.6	60	18.8

Note: Consumption of palatable biomass in g·m⁻²·yr⁻¹ was converted to a percentage of biomass consumed as applied in the model.

TABLE 3. Rules for the redistribution of R and P from vegetated cells for water-disconnected locations, wind-disconnected locations, and grazer-disconnected locations.

Slope position	Proportion moved from cell containing black grama			Proportion moved from cell containing creosotebush		
	East	Central	West	East	Central	West
Resource moved by water vector						
Up slope (north)	0.00	0.10	0.00	0.00	0.20	0.00
Central	0.10	0.50	0.10	0.05	0.50	0.05
Down slope (south)	0.05	0.10	0.05	0.05	0.10	0.05
Nitrogen moved by wind vector						
Up slope (north)	0.00	0.05	0.00	0.00	0.05	0.00
Central	0.15	0.50	0.15	0.05	0.45	0.05
Down slope (south)	0.05	0.05	0.05	0.05	0.30	0.05
Nitrogen moved by grazing vector						
Up slope (north)	0.10	0.10	0.10	0.0625	0.0625	0.0625
Central	0.10	0.20	0.10	0.0625	0.50	0.0625
Down slope (south)	0.10	0.10	0.10	0.0625	0.0625	0.0625

Note: Boldface values show the cell from which redistribution takes place.

are consumed (Hooper and Johnson 1999). When the loss of biomass is due to a deficit of nitrogen, the model allows the biomass to consume all resources in sufficient amounts to maintain (as far as possible) existing biomass. Under conditions of biomass loss, no propagules are generated. These rules reflect some of the observed adaptations of desert vegetation to survive extremes of climate (Walter 1971, McClaran and Van Devender 1995).

Descriptions of propagule movement are also inferred from literature. Although black grama provides excellent forage, populations are damaged by grazing as these plants rely heavily on stoloniferous regeneration (Canfield 1948, Gosz and Gosz 1996). While these means of reproduction are effective under arid conditions, they do not promote extensive migration. Consequently, black grama is slow to colonize adjacent areas (Brown and Gersmehl 1985). This effect is compounded by the low viability of its rarely produced seeds (Neilson 1986). The effect of droughts and grazing are to decrease tuft area, which allows for greater wind erosion of the upper loose soil litter layer required for stolon rooting. Creosotebush is a stable member of desert plant communities owing to its primarily vegetative method of reproduction via cloning (Cody 1986, Romney et al. 1989). Germination of seeds is rare, and the rate is reported to be less than

20% outside of the optimal summer rainfall of between 75 and 150 mm (Ackerman and Bamberg 1974). The seeds are primarily adapted for tumbling, as they are too heavy for lofting and the trichomes are not stiff enough to penetrate animal skin therefore not adapted to animal dispersal (Chew and Chew 1970).

In the model, we simplify these complex conditions of propagule production and movement by allowing propagules to be generated whenever a positive growth rate is recorded. For our purposes, propagules are a species-specific proportion of the new growth of each plant, and a proportion of these propagules is available to the vectors for redistribution within the environment. A small proportion of this annual new growth is allowed to move under the action of the vectors in the next time step, and will become established in new cells only if resource levels in these new locations are sufficient to support an increase in biomass. The majority of the propagules for each species will move to adjacent cells by diffusion to represent the predominantly asexual method of reproduction utilized by desert plants. If some propagules are moved to a connected cell, they are then dispersed along connected pathways by the vectors (Barbour 1969, Miller and Donart 1979).

For both species, water availability is the primary controlling factor in terms of propagule dispersal

TABLE 4. Summary of species demographic data.

Demographic data	Grass	Shrub	Data source
Maximum annual growth rate (%)	0.125	0.09	Peters (2002a)
Maximum biomass in 1-m ² cell (g)	319	222	Maneta et al. (2008)
Water efficiency ([g water]/[g biomass])	3.5	2.48	Peters (2002a)
Nitrogen use efficiency ([g nitrogen]/[g biomass])	0.6206	0.2767	Peters (2002a)
Water maintenance requirement ([g water]/[g biomass])	0.7	0.496	Peters (2002a)
Nitrogen maintenance requirement ([g nitrogen]/[g biomass])	0.125	0.055	Wainwright (2009)
Failure rate of species (% of species in cell)	5	5	
Mortality rate of species (% of species in cell)	10	10	

TABLE 5. Percentage of roots of the grass and shrub species that are distributed between the three soil layers.

Soil layer	<i>Bouteloua eriopoda</i> (%)	<i>Larrea tridentate</i> (%)
Top	13.3	6.7
Middle	50.4	32.0
Deep	36.3	61.3

(Aguiar and Sala 1999). This control is modelled by having the majority of propagules following the line of action of the water vector (i.e., downslope). These parameter values can be changed to account for the different germination probabilities of individual species, but for the simulations presented here, the values are fixed (Table 6). Species with seeds easily transported by the wind could be similarly moved in the model along the wind direction.

Descriptions of the simulations

The simulations have been carried out to test hypotheses of the different roles of precipitation and grazing in explaining woody shrub invasion and of the causes of spatial variability in response to drought. Conflicting results exist in the literature evaluating the effects of temporal variability in precipitation on vegetation. It is suggested that one cause of this conflict may be the consequence of the representation of the rainfall pattern in a model. To assess the extent to which this is the case, four simulations have been undertaken in order to explore different levels of complexity in the representation of rainfall on the resultant vegetation patterns and their interactions with grazing pressure. Simulations were characterized as follows: simulation a, stochastic rainfall with no temporal autocorrelation; simulation b rainfall reconstructed from the tree-ring record for the period 1659–1970; simulation c, same as b, but with variable grazing levels. For simulation a, the stochastic rainfall is generated from the mean and standard deviation of the reconstructed rainfall of simulations b and c. Finally, in simulation d, we use the model in conjunction with the 80-year measured rainfall-data record to examine reported differences in response to the same climatic conditions.

Initial conditions

All simulations were initialized from the same randomly generated landscape (Table 1), which included a random distribution of black grama biomass and a uniform distribution of shrub biomass (to represent a seedbank). An initial biomass of 60 g/m² was specified for black grama. This initial value was then perturbed by a low level of white noise (a random signal with a flat power spectral density, in this case, by generating a pseudorandom matrix of numbers lying between 0 and 1 with an average value of 0.5). This procedure follows the method of Coueron and Lejeune (2001). This method of perturbation of the biomass yields an initially random distribution of grass in each cell and the same initial

random distribution was used as a starting point in all of the simulations presented here. The initial biomass of the shrubs was specified as 10 g/m² in all cells, to represent a seed bank. The randomly generated map of biomass is depicted in Fig. 8. The initial resource level in the mid and deep layers was set to 25 g/m² for water and 0.25 g/m² for nitrogen. Resource levels of the top layer were provided by the input of water and nitrogen in each time step.

In all of the following simulations, all three vectors (water, wind, and grazers) operate to move R and P through the landscape. The effect of herbivory by grazers is included only in simulations c and d.

Presentation of results

We present the results of the simulations in two formats. In the first, we present three graphs showing the average change in grass and shrub biomass in the cells along a transect along the center line of the grid, the average change in water and nitrogen in mid and deep soil layers for the same cells, and changes in connectivity for these cells. In the second format, we display maps of grass and shrub biomass in each cell at selected times during the simulations.

RESULTS

Simulation a: stochastic rainfall

Results from Istanbuloglu and Bras (2006) have suggested that increased variability in rainfall and lower rainfall levels are mechanisms that, on their own and in combination with each other, will decrease the average grass biomass cover. This suggestion may be linked to the observation of Thornes and Brandt (1993), that more frequent woody plant encroachment and desertification are more likely to occur when the grass is in a

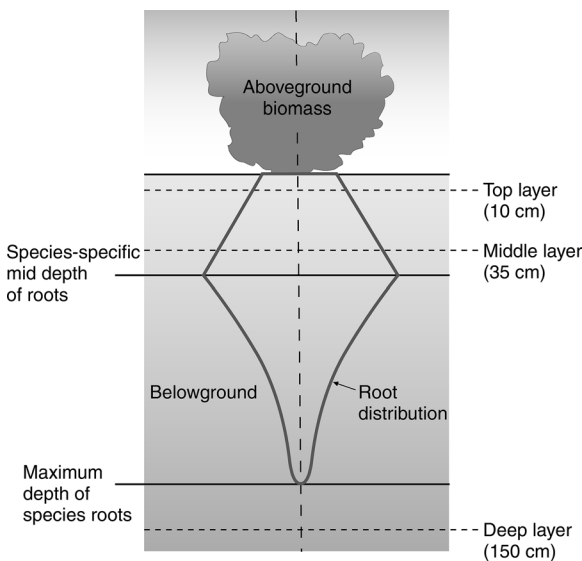


FIG. 7. Schematic diagram to show the distribution of roots in relation to the three soil layers in the model.

TABLE 6. Percentage of propagules for each species that is amenable to movement by the vectors.

Propagules	Vector (%)		
	Water	Wind	Grazer
Black grama	75	20	5
Creosotebush	85	10	5

degraded condition. Williams and Albertson (2006) argued similarly that some account must be taken of rainfall structure in models of dryland vegetation in order to understand the changes in a more meaningful way, (although they did not pursue this argument in their paper). For our first examination of the effects of rainfall (precipitation, p) representation on shrub invasion, we have reproduced Williams and Albertson's model, which controls the statistical structure of annual rainfall by generating a synthetic rainfall time series that is represented by the equation

$$Pr_t = \langle PR \rangle + UC_t + SA_p \sin\left(\frac{2\pi t}{T_p}\right) \quad (8)$$

where Pr_t is rainfall at time t , UC_t is an uncorrelated, log-normally distributed random variable with variance $\kappa\sigma_p^2$ where κ is a parameter lying between 0 and 1 that controls the partitioning of the total variance (σ_p^2) between uncorrelated (white) noise and correlated (sinusoidal) components (shown in Fig. 9a). SA_p is the sinusoidal amplitude (mm) and T_p is the period (years). The mean annual rainfall $\langle PR \rangle$ is the long-term average calculated from the tree-ring rainfall record as 228 mm/yr and the interannual variability of rainfall is represented by the coefficient of variance of rainfall ($CV[PR]$), which is calculated as 49.0%. The synthetic

rainfall fluctuates in values between years and has no periodicity within the rainfall structure (Fig. 9b). The simulation was run for the same length of time as the length of the reconstructed rainfall record.

The response of biomass in our model correspondingly shows wild fluctuations in values. Depending on the features of the synthetic rainfall series, either of the two species is equally likely to become the dominant biomass in the grid without any bias toward the grass or the shrub. In the realization of the stochastic model shown in Fig. 10a, the grass and shrub continually alternate as the dominant species, and neither species shows any evidence of spatial reorganization.

When the grass is the dominant species in a cell, little available resource migrates to the deeper soil layers (Fig. 10b). However, when the shrub is the dominant species, a large amount of water resource is channeled to the deep layers. Transitions between one dominant species and another are accompanied by a change in connectivity (Fig. 10c). When a drought occurs, the biomass of both grass and shrubs is reduced, and when rainfall subsequently increases the grass and the shrubs both increase their biomass. The principal difference between the two plant species during recovery is growth rate. As the grass has a higher growth rate, it can recover slightly more quickly than the shrubs and suppress shrub invasion. In this sense, the variability in the rainfall itself inhibits shrub invasion, and confirms that the periodicity in rainfall is an important control on vegetation response.

Simulation b: reconstructed rainfall

For this simulation, the actual 312-year rainfall series that was reconstructed from tree-ring data was used. Results of same center-line averages as in Fig. 10 are

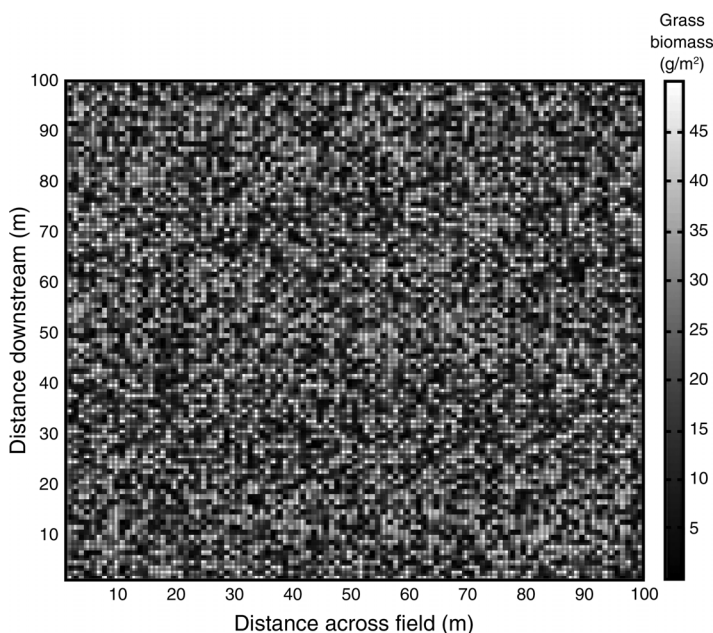


FIG. 8. The randomly generated initial conditions for the model runs.

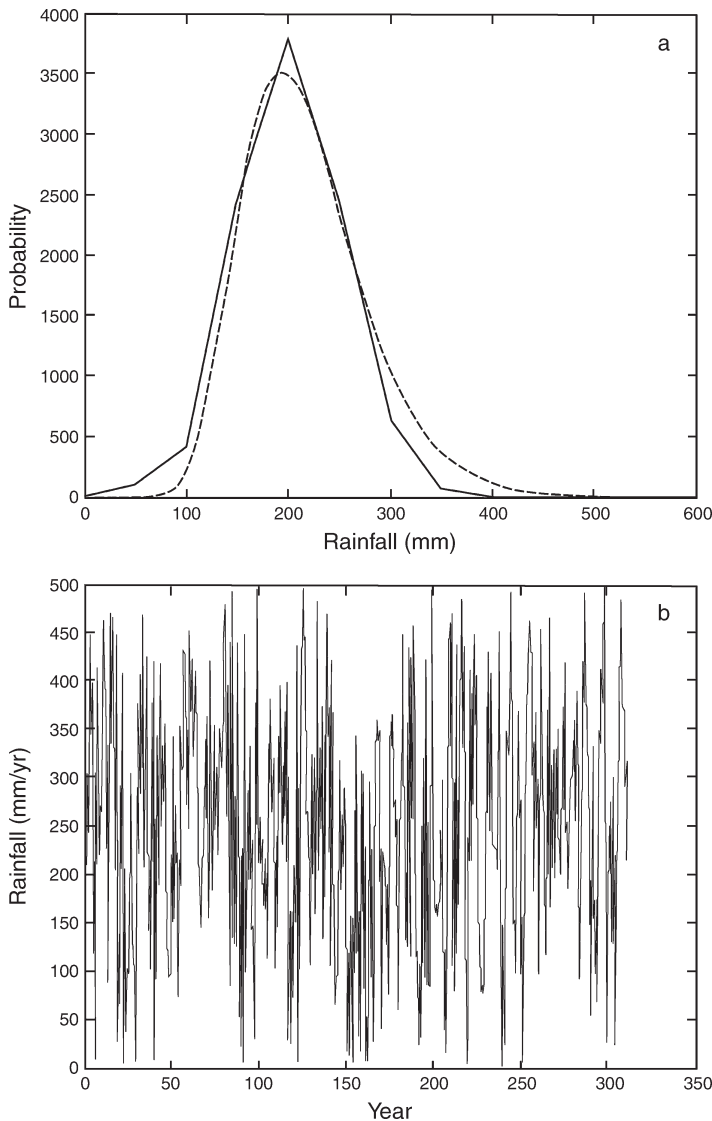


FIG. 9. (a) Lognormal probability distribution (shown by the dotted line) to approximate observed rainfall (shown by the solid line) at the Jornada LTER. (b) Example of the resulting stochastic rainfall model.

presented in Fig. 11. The initial decline of grass biomass is caused by initiating the calculation with uniform resources in the mid and deep soil layers. Over the first 25 years of the simulation, the biomass adjusts to these arbitrary resource levels, and so these first few data points are excluded from further analysis. Fig. 11a shows that after this initial period, although the average value of grass fluctuates, the shrubs are unable to become established.

It is noteworthy is that even after the most extreme drought (that of the 1950s), the grass population is able to recover and the shrub population continues to be suppressed. It is not unreasonable to expect that the same recovery of grass should be observed if droughts of a similar magnitude occurred at earlier points in the simulation (c.f. McClaren and Van Devender 1995), assuming that the reconstructed data underestimate the magnitude of earlier droughts (see *Model implementa-*

tion: Model parameterization: Externalities and vertical processes).

The middle-layer water resource fluctuates markedly (Fig. 11b). As the average grass biomass increases, water levels decrease and vice versa. In spite of the accumulation of the water in this layer, the shrubs are not able to invade, which, assuming our model is faithfully reflecting the impacts of rainfall variability, suggests that some other mechanism apart from drought must be important in shrub-invasion processes.

Connectivity (Fig. 11c) also fluctuates during the simulation. The average connectivity values show that whereas the magnitude of change in the grass population reflects the magnitude of change in the rainfall record, the response of the grass population tends to lag slightly behind changes in the rainfall (typically by two years). The lag is partly due to the unused resource being moved down through soil layers, and partly due to the structure

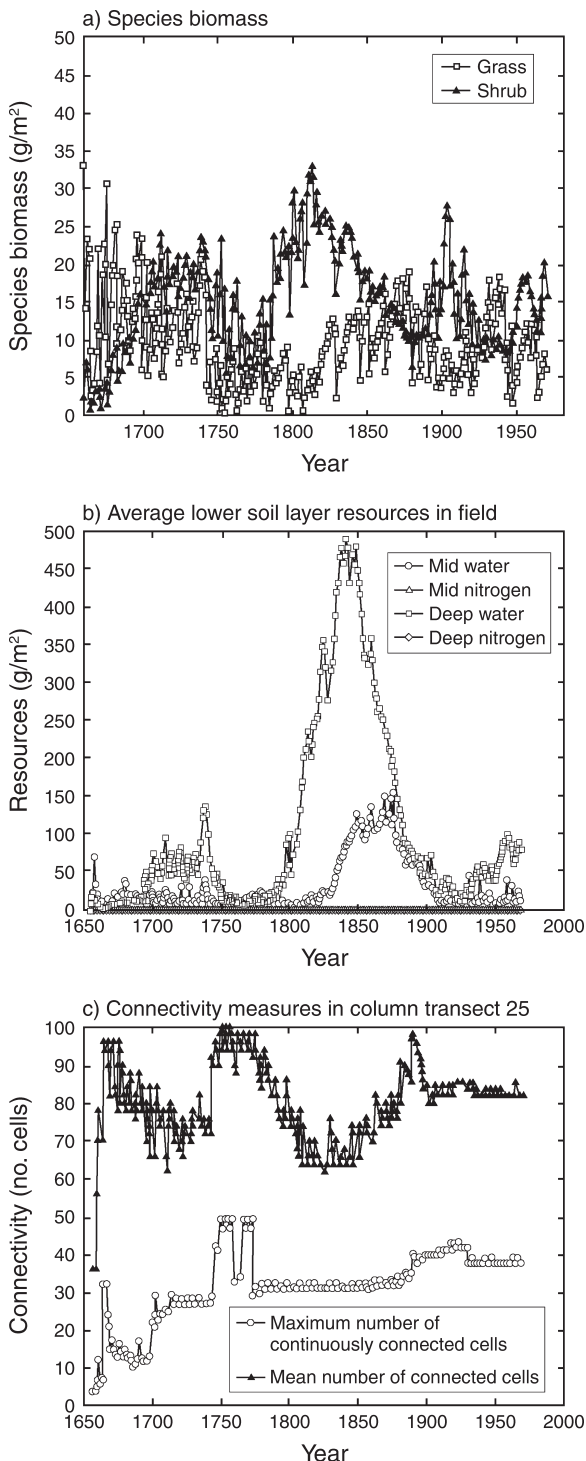


FIG. 10. (a) Biomass of grass and shrubs, (b) water and nitrogen levels in the mid and deep soil layers, and (c) connectivity with respect to the water vector for the 50 cells along the center line of the grid for each year of the 312-year stochastic rainfall simulation. Values are means. Note that, because the rainfall record is stochastically generated, individual model realizations may differ substantially. However, all models that we have run show no long-term spatial reorganization of the vegetation.

of the rainfall in the sense that multiple wet years will increase patch biomass, which delays the effect of subsequent dry years on population decline (and vice versa). Although this delay may in part be an artefact of the calculation scheme, it is not inconsistent with the observations of the actual behavior of the system as evaluated by Reynolds et al. (1999). The maximum number of connected cells also changes, related to a change in the spatial organization of the grass patterns. Therefore, the implication is that the temporal structure of rainfall plays a significant role in the spatial organization of vegetation, as well as its dynamic response.

In order to examine the changing spatial distributions of the biomass, maps of the distributions of grasses and shrubs are shown in Fig. 12. The biomass of grass decreases during times of water scarcity in a consistent and predictable way. During dry years, grass is first lost from cells containing the lowest biomass. These cells connect to the wind and water vectors and resource “flows” into the next vegetated (i.e., disconnected) cell. This flow has the effect of concentrating resource into distinct spatial locations and allowing a higher biomass of grass to survive than would otherwise be possible were the resources more homogeneously distributed (Humphrey 1958, Buffington and Herbel 1965, Allred 1996, Couteron and Lejeune 2001, Barbier et al. 2006). At first, the vegetation loss occurs only in the lowest biomass cells. During prolonged periods of water stress, vegetation is lost from the downslope edge of the vegetation patch, because the water input provided by the vector is exhausted before it reaches this edge and consequently a “banded” pattern is formed (e.g., noted in years 1783–1883). As noted in the Appendix, this banded pattern that is widely reported in the literature on desert vegetation. Over time, these bands become more fragmented. When the water input is increased, grass recovery initiates from all surviving grass cells. The relationship between the number of connected cells and the width of the grass band is a function of both the resource input and the biomass of the band.

Meanwhile, the shrub biomass declines (as suggested by Goldberg and Turner 1986) and by the time grass reaches its quasi-average value the initial shrub biomass has been reduced to an average value of almost zero. Where shrubs are able to survive, they do so only on the edge of a grass patch which has accumulated excess resources, and in effect, the grass patch acts as a nurse plant to the new creosotebush (McAuliffe 1988). This quasi-static equilibrium level for the grass controls the resource and propagule movement, by which it is meant that the pattern of resource movement in this simulation is predominantly lateral, locally limited, and observed in the top layers on the same spatial scale as the individual grass plants (Müller et al. 2008). This result is consistent with evidence that the dominant species redistributes resource to suit its own colonization strategy, which has been noted by Westoby et al. (1989).

The grass never quite reaches a stable equilibrium, irrespective of the duration of the simulation. Model runs of 1000 years were also carried out using both repetitions of the stochastic rainfall record and repeated cycles of the tree-ring record. In these model runs the grass population did not get any closer to reaching a steady equilibrium, which allows the idea that equilibrium is asymptotically reached, given an infinitely long time, to be rejected.

Simulation c: reconstructed rainfall and variable grazing levels

Simulations a and b indicated that the temporal structure of the rainfall is a causal factor leading to the generation of patchy vegetation, but the results also suggest that historical climatic conditions appear to be insufficient to cause the invasion of shrubs into grasslands. The introduction of grazers to the Jornada has often been cited as a reason behind woody plant encroachment (e.g., Archer et al. 1995) and so, in this simulation, the variable rainfall input is combined with three different grazing intensities. These grazing levels are modelled as a disturbance externality by allowing some of the grass in each cell (as a percentage of the maximum cell biomass) to be removed. This percentage corresponds to the mid-point of three grazing intensities reported for the Jornada (Table 2).

Fig. 13a shows that, with a conservative grazing intensity, the average biomass, resources, and connectivity are little changed compared with simulation b (mean average grass and shrub biomass 30.6 g/m² and 0.4 g/m², and 27.5 g/m² and 0.6 g/m², respectively) where the effects of herbivory were not simulated (although the grazing vector did operate to move R and P in simulation b). Although average grass biomass levels (Fig. 13b) are reduced in the simulation with recommended (Havstad et al. 2006) compared with the conservative grazing intensities, there is little difference in the average shrub levels (mean average grass and shrub biomass, 27.5 and 0.6 g/m², 27.8 and 0.6 g/m², respectively). The connectivity values (Fig. 13g-i) show that under recommended grazing levels, the effects of droughts become more pronounced with a greater number of cells connecting to the wind and water vectors, and the average connectivity suggests different spatial patterns in the vegetation occurs in response to the elevated grazing levels (maximum continuous connected cells 38 and 38, respectively, and average connected cells 4.6 and 5.6, respectively). The over-grazed simulation (Fig. 13c, f, i) produces conditions that result in a dramatically reduced grass biomass and a much high higher average shrub biomass (18.7 and 10.6 g/m², respectively). The effect of the increased shrubs is also seen in the average resource levels (Fig. 13f) where greater levels of water resources are able to penetrate the deep soil layers (different spatial scale arguments). By the time that the drought of the 1950s occurs, the biomass of the shrubs exceeds that of the grass (Schle-

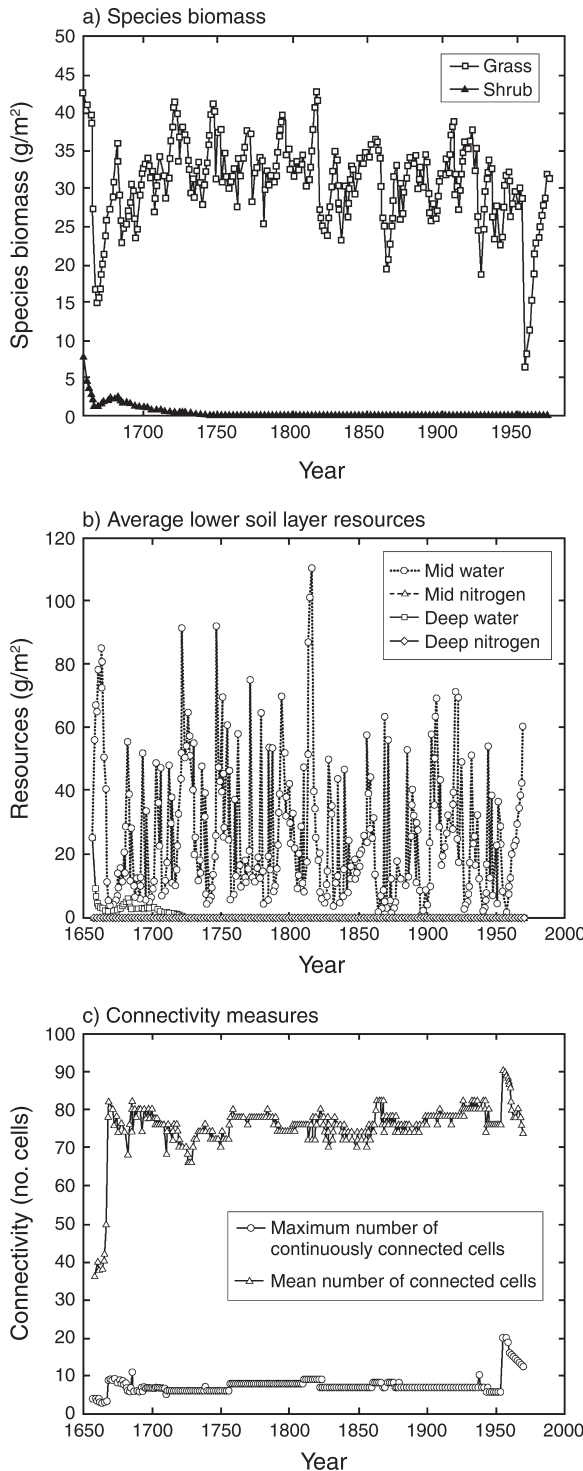


FIG. 11. (a) Biomass of grass and shrubs, (b) water and nitrogen levels in the mid and deep soil layers, and (c) connectivity with respect to the water vector for the 50 cells along the center line of the grid for each year of the 312-year reconstructed-rainfall series simulation. Values are means.

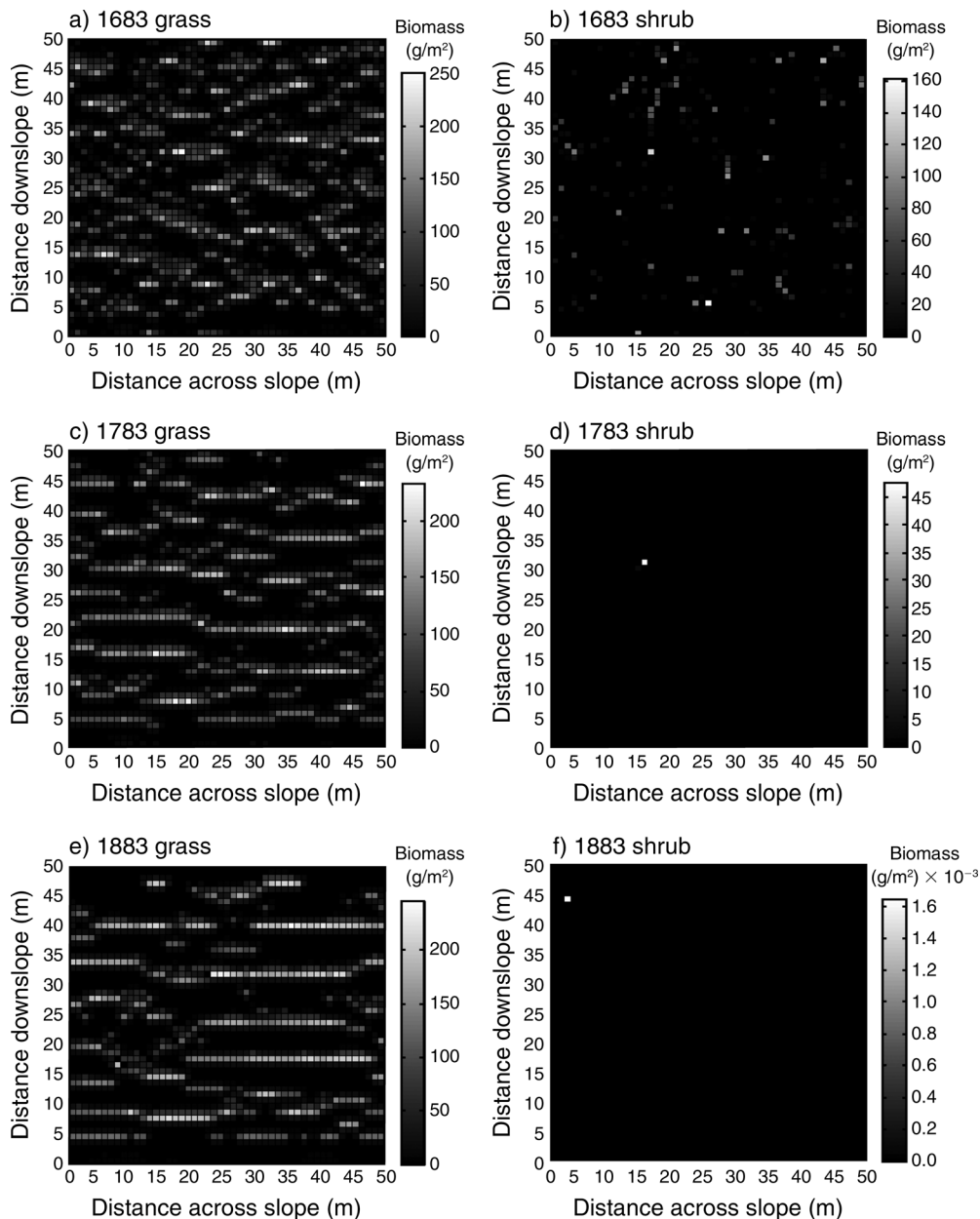


FIG. 12. Maps depicting the spatial distribution of grass and shrub biomass in years 1683, 1783, 1883, 1958, and 1970 for the reconstructed-rainfall series simulation.

singer and Pilmanis 1998). In spite of this change, the connectivity values (Fig. 13i) imply a very static pattern in the spatial pattern of biomass.

In order to interpret the patterns of connectivity in the overgrazed case (Fig. 13i), the spatial patterns of biomass for the overgrazed case are shown in Fig. 14. It can be seen that the typical banded pattern is established early in the simulation. The resources that are moved by the vectors should be able to sustain a high level of grass in the disconnected cells (as in simulation b); however, the grazers remove some of this

biomass. What would have been adequate resource becomes an excess resource on these grass patches, and the shrubs are able to colonize these areas of resource excess. Once the shrubs have become established in the locations shown in Fig. 14, the model identifies them as the dominant species, which has two consequences. First, the diffusion descriptions (Table 3) pertaining to shrubs are used in place of the diffusion descriptions for grass. Second, the shrubs are allowed to channel some of the water input to their cells directly to the middle and deep soil layers. At this point, the resource redistribution

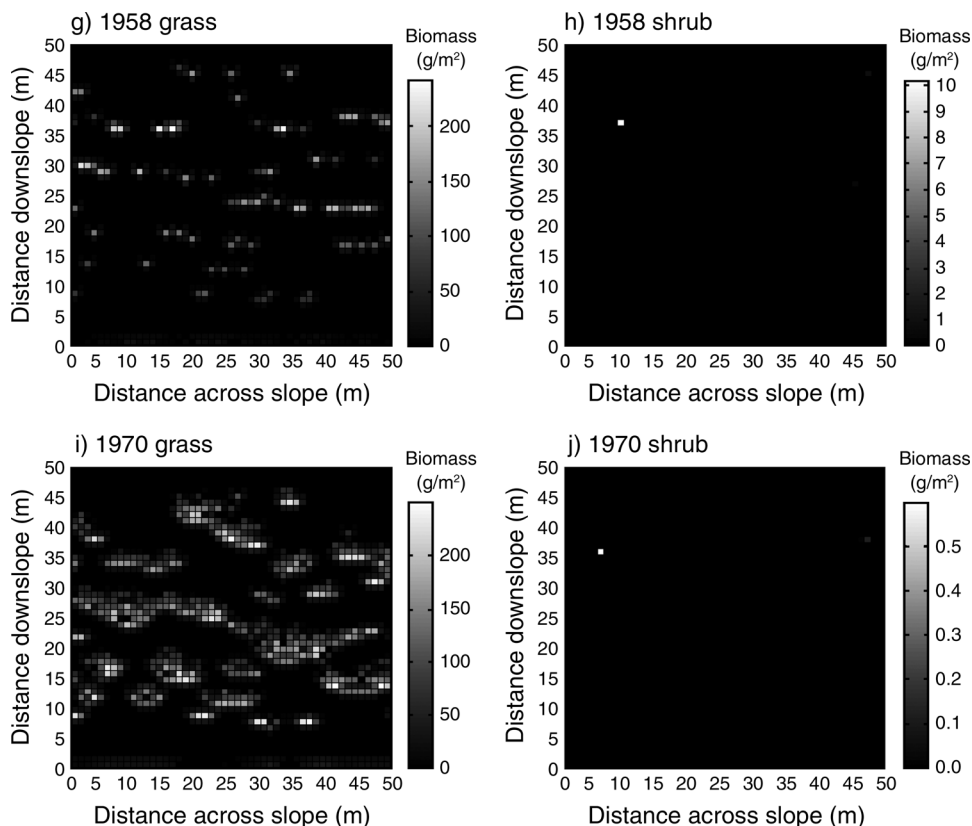


FIG. 12. Continued.

changes from a predominantly lateral process (where resources move to adjacent cells in the top soil layer) to a more vertical process where the shrubs are able to channel a higher proportion of water resources directly into deeper layers. During times of resource scarcity, these shrub patches contract and shrub biomass is reduced, but they are to some extent buffered from the effects of water shortage by the deep-water store (Thornes and Brandt 1993). Thus the shrub community is quite stable, and therefore the spatial distribution of biomass and connectivity values also become more static. In the earlier simulations, the grass community was able to adapt to resource scarcity by expanding and contracting in patches as a function of connectivity. In the present case, the shrub population interrupts this connectivity and the grass patches become increasingly fragmented. At the end of the simulation, most of the grass survives only at the edge of the shrub patch (as observed in the field by McAuliffe [1988]).

Simulation d: measured rainfall data and a conservative grazing level

Reynolds et al. (1999) and Yao et al. (2006) reported that different sites within the Jornada Basin have responded differently to the same climatic conditions: some stands of perennial grass became extinct before the drought of the 1950s, some during the drought, some

immediately afterward, and some not at all. Yao et al. (2006) used long-term cover data over a period from 1915 to 2001 to identify this spatial variation in grass cover in the Jornada and, in the absence of a consistent causal factor, hypothesized that local transport processes for resources and propagules between patches must be somehow be important. In this simulation, we use 80 years of measured rainfall data to generate simulated grass responses in order to explore the model's ability to test Yao et al.'s hypothesized explanation. Unlike previous simulations, the initial conditions for this simulation (in terms of middle and deep soil layer resources and biomass distribution) are taken from the results obtained at year 1915 of the previous simulation using the reconstructed rainfall series in order to avoid, or at least minimize, the effects of adjusting to initial resource redistribution. Yao et al. (2006) reported a low (conservative) grazing level applied on their quadrats over the period from 1915 to 2001, which was calculated from averaged monthly stocking data that also accounted for changes in fence positions. We therefore apply the same conservative grazing level following the management strategies evolved by the Research Station over this period (Havstad et al. 2006).

The center-line averaged results are presented in Fig. 15, where it can be seen that the grass biomass follows (but lags behind) the rainfall pattern (Fig. 5a). The

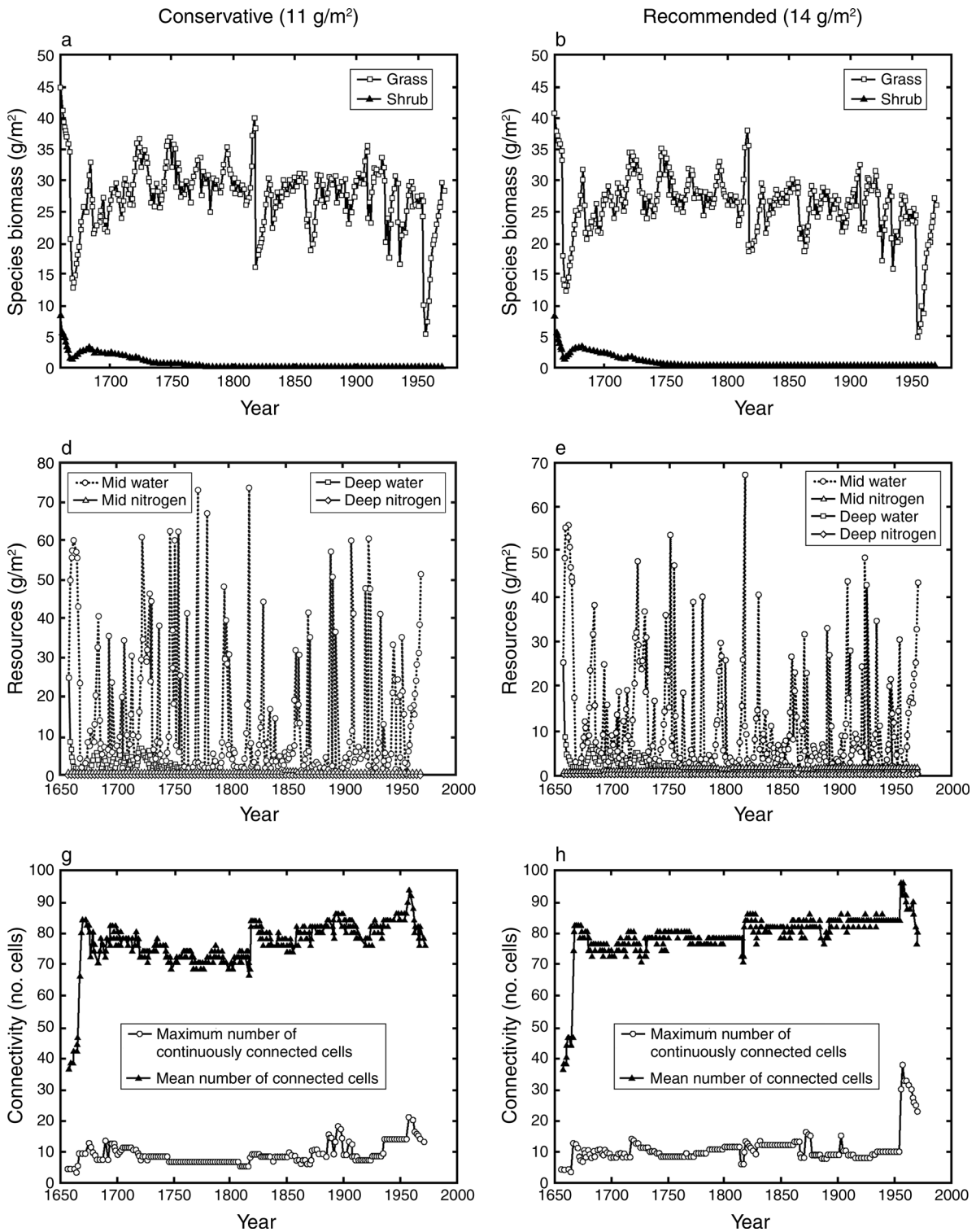


FIG. 13. (a–c) Biomass of grass and shrubs, (d–f) water and nitrogen levels in the mid and deep soil layers, and (g–i) connectivity with respect to the water vector for the 50 cells along the center line of the grid for each year of the 312-year reconstructed-rainfall series simulation, for (a, d, g) a conservative grazing level (11 g/m²), (b, e, h) the recommended grazing level (14 g/m²), and (c, f, i) the overgrazed case (45 g/m²). Values are means.

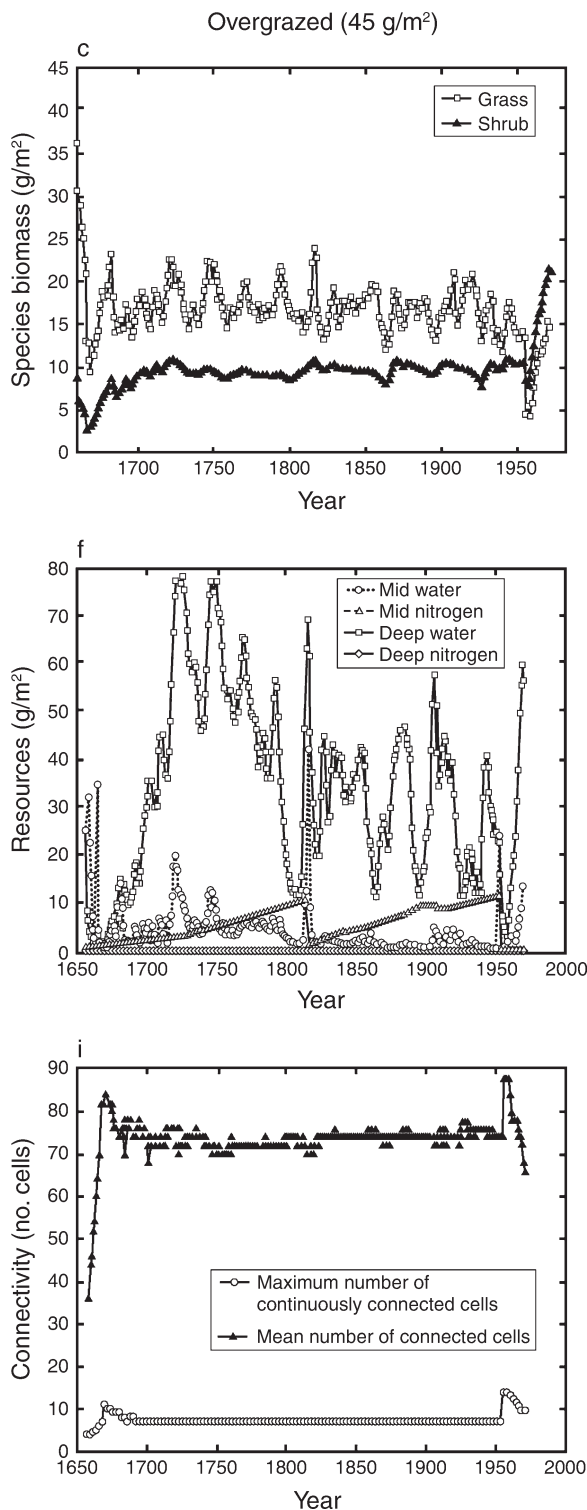


FIG. 13. Continued.

average shrub biomass is low, but remains above zero due to the grazing disturbance. The wetter years following the 1950s drought allow an accumulation of middle and deep-layer soil resources, and a trend for average connectivity values to increase is also evident. An increase in connectivity may indicate that the spatial distribution tends toward a more open plant community (Okin et al. 2001), or that there is an increase in spatial organization of the plant community.

The spatial distributions of the grass and shrubs are plotted in Fig. 16. The increasingly fragmented pattern in the grass distribution becomes apparent during the dry years of the 1920s and 1930s, as a result of the persistence of shrubs (compare maps for 1925 and 1935). The recovery process of both species is particularly well illustrated in the results for 1965, 1975 and 1985. During the drought of the 1950s, the shrubs persist as isolated spots, whereas the grass survives as short horizontal bands (orientated across the slope). As the grass recovers, these bands extend laterally, and then coalesce to form longer and more continuous bands, while the shrubs recover to form isolated communities that are orientated in the direction of the driving flux (shown also in Fig. 14). This pattern is caused by the shrubs' requiring longer connected pathways than the grass (the length of this pathway is again a function biomass and resource input) and because R and P diffusion around the shrub is vertical (through the soil layers) as well as lateral.

The contraction and recovery of biomass is also shown by plots of biomass and resource concentration (Fig. 17) that are plotted for the center line. In 1925, cells with high grass biomass are interspersed with cells with low biomass. Shrubs exist on the edges of these grass peaks, and water resources are concentrated onto the grass patches. Following the drought and subsequent recovery during the 1930s, the number of grass cells is reduced, and in some places, the shrubs have recovered to higher biomass levels than those observed for the grass. This recovery happens where the vectors move excess resource to a patch, which then loses some biomass by drought or disturbance.

During the severe drought of the 1950s, most of the biomass is lost except in the locations that contained the highest biomass prior to the drought, and recovery initiates from these cells during the 1960s. From this point on, the surviving biomass exists at higher concentrations, but in fewer cells. Resources are concentrated in patches, which are interesting in a number of ways. First, the concentrations are at levels that greatly exceed the resource input to the grid. Second, they exceed the resource requirement of the grass. Third, they also exceed the level that can be consumed, even under the maximum growth rate for the grass (Table 4). The concentration of resources into patches supports a higher biomass than the same resource could support, were the grass more homogeneously distributed (as suggested by Aguiar and Sala

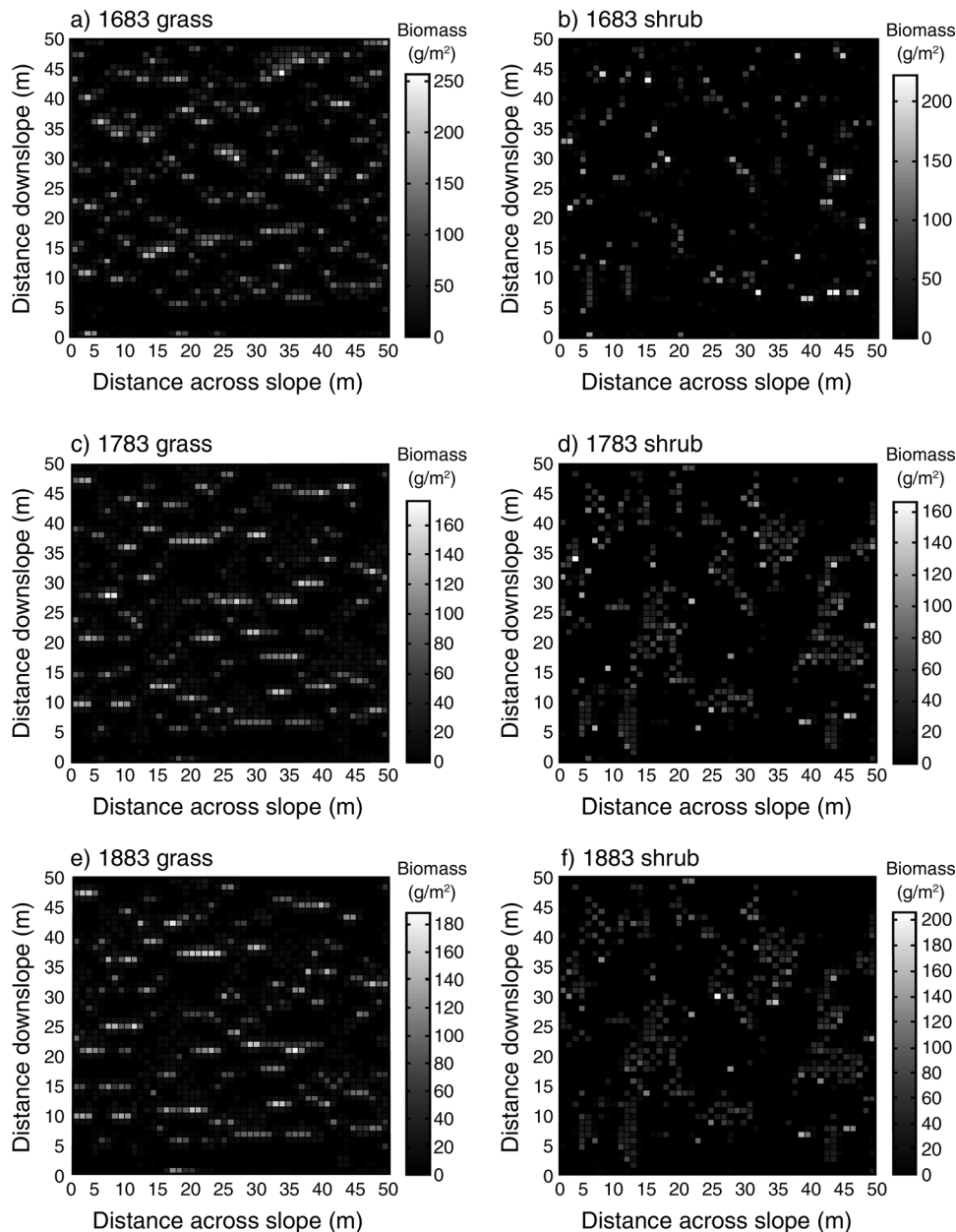


FIG. 14. Maps depicting the spatial distribution of grass and shrub biomass in years 1683, 1783, 1883, 1958, and 1970 for the overgrazed grazing simulation.

[1999] and Barbier et al. [2006]). It can be noted that the biomass on the up-gradient edge of the band is higher than at any point earlier in the simulation on a more uniform grid (as observed by Ludwig et al. [2005]).

Inspection of the resource transects show that for similar (and fairly static) banding patterns, the distribution of subsurface resources can be very different from each other. On the transect (Fig. 18), the shrubs are ultimately suppressed by the grass, but elsewhere in the grid, some shrubs cells are able to survive. Two conditions are met by the surviving shrub cells. First,

they are those that contained a high pre-drought biomass. Secondly, these shrub cells are located on the edge of a surviving grass band (McAuliffe 1988). This pattern occurs because the grass bands are able to concentrate resources to an extent that exceeds their maintenance and maximum growth-rate requirements. The shrubs can capitalize on this excess resource, but elsewhere, any surviving shrubs that do not lie on the resource bands die off, even where the initial pre-drought shrub density was high (Schlesinger et al. 1990). Whether or not shrubs will survive after the drought

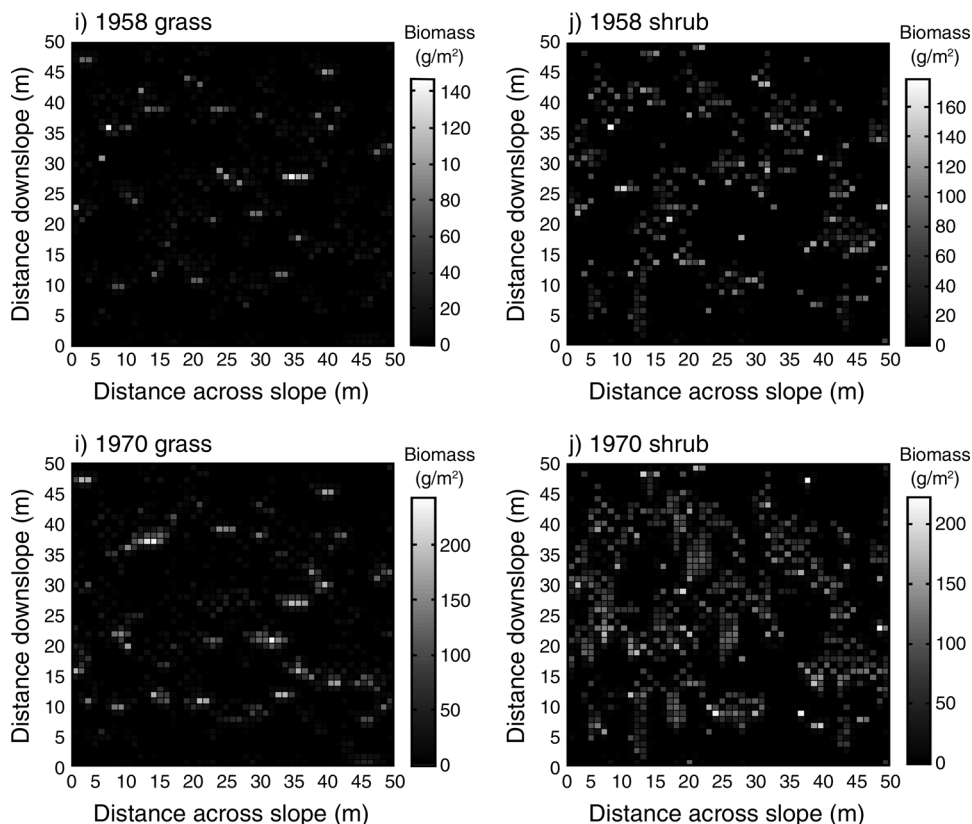


FIG. 14. Continued.

(during times when resource inputs are increased and grass populations recover) is a little more complicated. Even with a sufficiently long connected path, shrub cells will not persist in locations where resource movement is controlled by the grass, i.e., predominantly lateral. In order to persist the shrubs also require sufficient vertical input of resources that can be channeled to the deeper soil layers (a process documented in the literature, e.g., Martinez-Meza and Whitford [1996], and included in the model). This result points toward the importance of different pathways of resources movement occurring within the shrub populations, specifically a vertical connection between water input and deep layer soil resources (which could be considered as a type of connectivity).

In Fig. 18, the experimental data of Yao et al. (2006) are compared to simulated data from cells selected manually from the transect of Fig. 17 that show a similar response to Yao et al.'s data. The selected simulated responses show markedly similar trends, although the specific values are different. This difference most probably arises because the experimental data measured the area covered by a plant in each quadrat to evaluate basal cover, whereas the model computes biomass.

In the first example (Fig. 18a and b), where grass is lost during the early 1920s, the biomass of this cell was

lower than in neighboring cells, and so biomass was shed from this cell very quickly. A number of upslope cells subsequently became connected, and the biomass increased slightly as a result of the extra resource input, before becoming extinct in 1924. After grass was lost from this cell, the number of upslope connected cells continued to increase. Without any nearby surviving patches to exchange resource and propagules with, this cell remained empty for the remainder of the simulation (Fig. 17).

The second example (Fig. 18c and d) shows the biomass response of a cell where grass was lost during the drought of the 1950s. Initially, this cell was toward the downslope edge of a grass patch. Grass persisted for a time on this patch while upslope cells were connected to the vectors. A consequence of this increased connectivity was that new growth appears to have occurred on the upslope edge of this cell and biomass was progressively lost on the downslope edge of this band during periods of climatic stress. During the drought of the 1950s, there was insufficient resource added by precipitation to sustain the biomass in this cell and the additional resource that was delivered to the patch by the vectors was consumed by upslope biomass before it could reach the cell. Consequently, grass in this location was lost. It is worth noting that toward the end of the simulation, the grass in this cell is able to recover

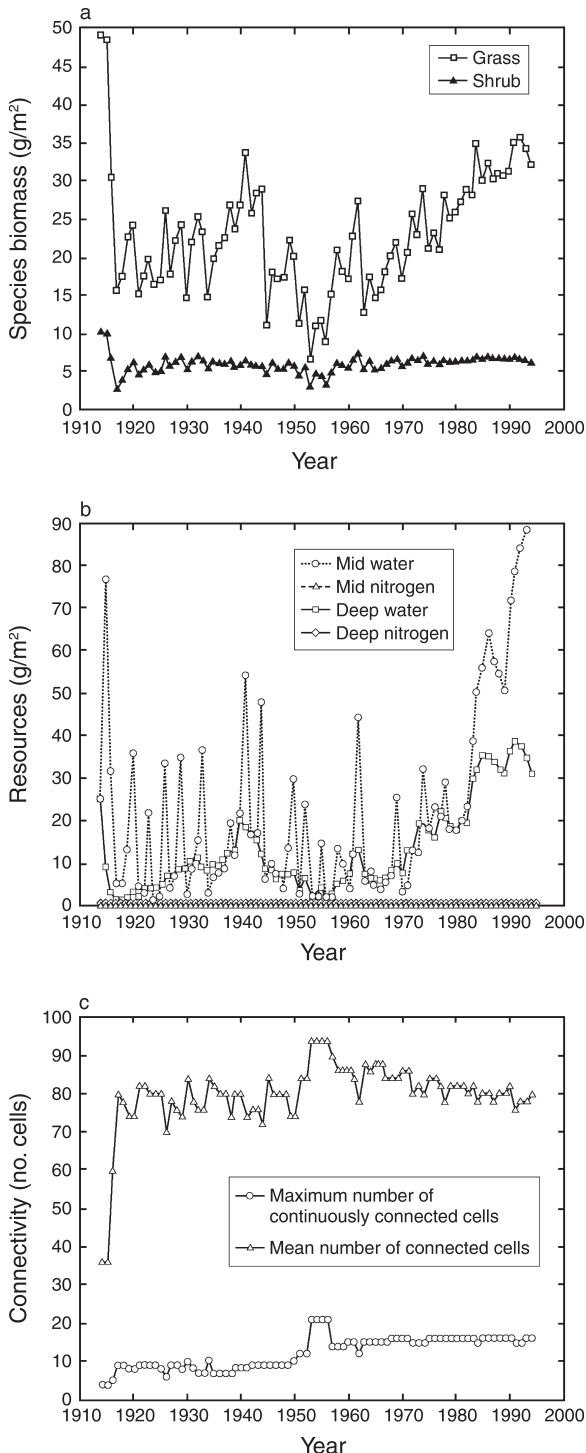


FIG. 15. (a) Biomass of grass and shrubs, (b) water and nitrogen levels in the mid and deep soil layers, and (c) connectivity with respect to the water vector for the 50 cells along the center line of the grid for each year using the measured rainfall record and a conservative grazing level. Values are means.

most likely because this simulation does not account for concomitant soil degradation, which almost certainly occurs. This recovery is not observed in the data of Yao et al. (2006).

The third example (Fig. 18e and f) shows a cell where grass was lost immediately following the 1950s drought. This cell is located immediately upslope of the cell in the second example, and the processes applying in the two locations are the same. The difference is that this cell is located further toward the center of the grass patch and survives for longer. After the drought, the upslope biomass was able to increase quickly in response to higher rainfall inputs and higher water input by the vectors. This rapid growth inhibits the recovery of this cell and ultimately grass is lost in this location, immediately following the drought. Elsewhere in the grid, an upslope shrub cell has the same effect, in that it interrupts the connectivity to the grass cell.

The final example (Fig. 18g and h) shows a cell where grass has survived throughout the duration of the simulation. This cell exists near the upslope edge of a grass patch (cf. Montana 1992) and as such it has received high water inputs from upslope connected cells, even during the droughts, and its connectivity was not interrupted following the drought.

Yao et al. (2006) reported data from 98 1-m² quadrats in the Jornada, and reported that black grama became locally extinct on 21% of these plots prior to the 1950s drought, 39% during the drought, and 30% after the drought, and the grass persisted throughout the time of study in the remaining 10% of quadrats that were examined. Simulation d generated biomass data in 1-m² cells, using a parameterization consistent with the location of the data of Yao et al. In simulation d, black grama became locally extinct in 26% of the cells prior to the 1950s drought, 38% during the drought, 20% after the drought, and black grama persisted in 16% of the cells. The simulated and measured results show remarkably good agreement with each other, with the largest differences occurring after the 1950s drought where simulation d overpredicts the number of cells where grass survives. This overprediction may be because there is no mechanism within the model that would allow for a spatial location to be degraded by hillslope processes during a disturbance and therefore inhibit biomass recovery (Montana 1992, Abrahams et al. 1995).

DISCUSSION

In the early part of this paper, we have argued that, though modelling can provide unique insights into understanding the dynamics of the patchiness of desert vegetation, such insights are valuable only if models yield testable predictions and if the models are firmly grounded in, and compatible with, empirical data. That is not to say that empirical data are uncontestable. All data are collected within a conceptual framework, and it may be that modelling will yield results that lead us to challenge that conceptual framework. Even so, such a

challenge is only valid where the model makes explicit reference to that conceptual framework. Against that argument, we have developed a numerical model for the dynamics of desert ecosystems within the conceptual framework of connectivity, and we have parameterized the model for implementation in a specific desert setting where the available data set for parameterization is particularly rich. In this section, we discuss the model output in terms of its ability to generate testable hypotheses.

Four testable hypotheses emerge from our modelling of shrub invasion of grasslands. First, our results show that, contrary to Thornes and Brandt (1993), rainfall variability does not enhance shrub invasion. Instead, because the annual regrowth rate of grass rate is higher than that of shrubs it recovers faster and is thus able to suppress shrub invasion by reestablishing its control on resource redistribution. This result suggests the hypothesis that the propensity of a grassland for shrub invasion is a function of the relative growth rate of the two. It should be noted, however, as a caveat to this hypothesis there may be extremes of drought beyond those tested here under which such a control breaks down.

Second, Yao et al. (2006) hypothesized that control by transport processes on local resource and propagule distribution may somehow explain the spatial variation in grass survival within the Jornada Basin. Our analysis suggests that the timing of grass loss depends on both initial cell biomass and connectivity properties. Low biomass density patches will always become extinct first during times of resource shortage. During prolonged periods of drought, biomass on the downslope edge of a patch is the most vulnerable, particularly if a shrub exists nearby, because the shrub will channel some of the resource input to deeper layers and so a longer connected pathway or a greater resource input is required to supply the grass cell than would be required if the shrub were not located nearby. Cells that lose biomass tend to have low numbers of upslope connected cells. Patches that survive drought conditions are those that are located near the upslope edge of the patch, where there is a high degree of connectivity in up-vector cells. These results lead us to suggest the hypothesis that changes in the values of connectivity for grassland indicate conditions where it would be particularly vulnerable to a disturbance externality.

Third, our results lead us to hypothesize that when the grass species becomes established and forms a stable community, it is able to control the resource and propagule movement within the landscape to suit its own survival strategy. In the case of pure stands of grass, this hypothesis means that the resource distributions coincide with the scale of grass plants, and underlying resources in deeper layers are at a minimum (Müller et al. 2008). When conditions change to allow deeper layer resources to accumulate, shrub invasion into a grass stand can occur. This hypothesis therefore predicts a vertical resource gradient should occur

beneath shrub communities, whereas the resource gradient surrounding grass patches should be predominantly lateral. These predictions are supported at least qualitatively by the results of Schlesinger et al. (1996). The simulations also suggest that a vertical resource profile could be an independent means by which the islands of fertility model can be tested. Furthermore, it has been argued that under conditions (that are usually driven by a strong externality) where the dominant grass species has collapsed, permanent changes in soil condition (such as caused by erosion, as noted by Westoby et al. [1989], Abrahams et al. [1995], Li et al. [2007]) would become much more important and are likely to inhibit future vegetation establishment in eroded areas (Wainwright et al. 2000, Okin et al. 2006, Li et al. 2009). Mauchamp et al. (1993) theorized that stripes are controlled by different recruitment histories, and that on a landscape scale it is the successive die-back and regrowth that controls stripes. Because our model only allows these different recruitment processes to occur in response to resource inputs, and because we are, nevertheless, able to generate plausible results, it leads to the hypothesis that resources rather than changes in soil conditions per se that are the primary controlling factors.

Fourth, the distinct differences in our modelling results between diffusion–advection and advection-only simulations (see Appendix) lead us to hypothesize that the balance of these two sets of processes and the nature of diffusion play a large part in controlling vegetation behavior. It would be possible to test this hypothesis by conducting field experiments in which the ability of vectors to move resources and propagules in these ways was examined.

That our model is able to generate specific testable hypotheses is due to the specific parameterization that we have been able to provide for the data-rich Jornada Basin. However, the relationship between the utility of a model and the available data for parameterization is not a simple one. Where such data do not exist, a model may be used to identify specific data needs for testing of hypotheses. Sensitivity of model output to particular parameters can drive empirical research just as much as the results of empirical research can lead a model to produce testable hypotheses. For example, key parameters in understanding the process of shrub invasion and the potential for its reversal are the rates of establishment and mortality for creosotebush. Current estimates for these parameters are derived from other modelling studies (Peters 2002a), suggesting that further empirical work is needed to constrain the potential values of parameters to which the model is highly sensitive.

CONCLUSIONS

In this paper, a modelling framework that explicitly considers spatial interactions among multiple vegetation types and multiple resources has been applied to the analysis of ecosystem change in deserts. The model is

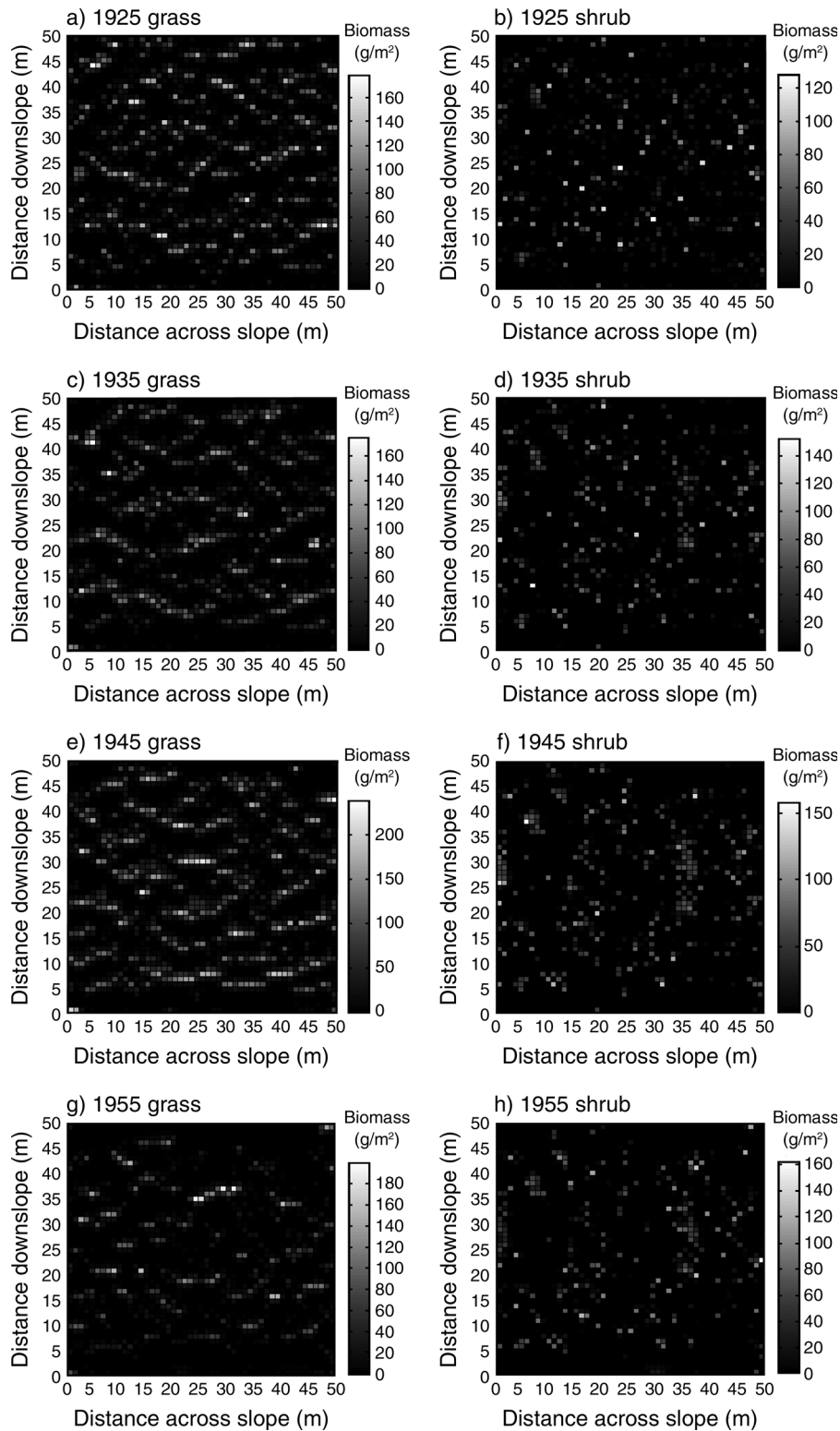


FIG. 16. Maps depicting the spatial distribution of grass and shrub biomass at 10-year intervals for the simulation using the measured rainfall record and a conservative grazing level.

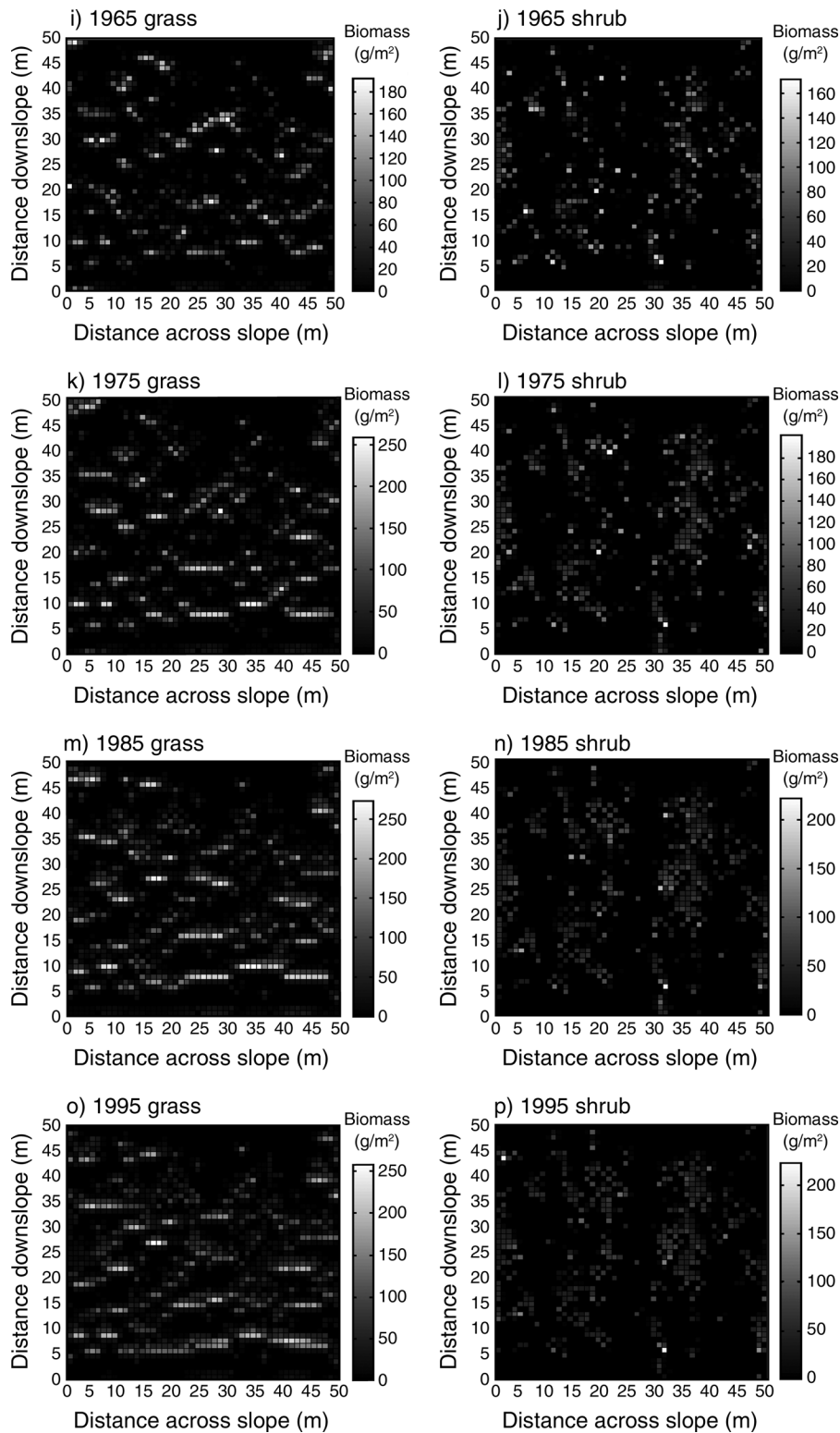


FIG. 16. Continued.

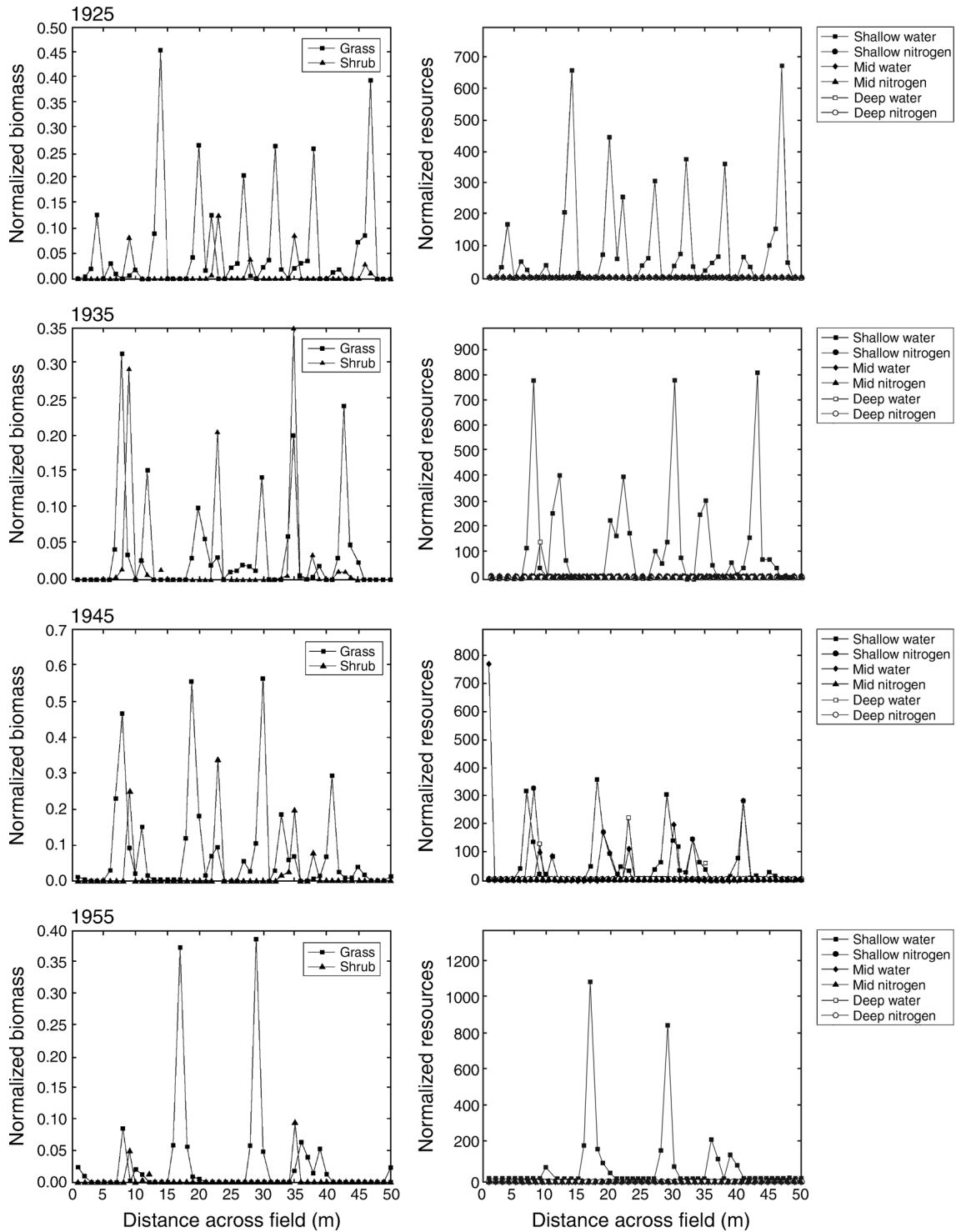


FIG. 17. Biomass and resource distribution along the center line of the grid at 10-year intervals for the simulation using the measured rainfall record and a conservative grazing level. For ease of representation, modeled biomass and resource density are scaled (normalized) to the maximum potential biomass given in Peters (2002a).

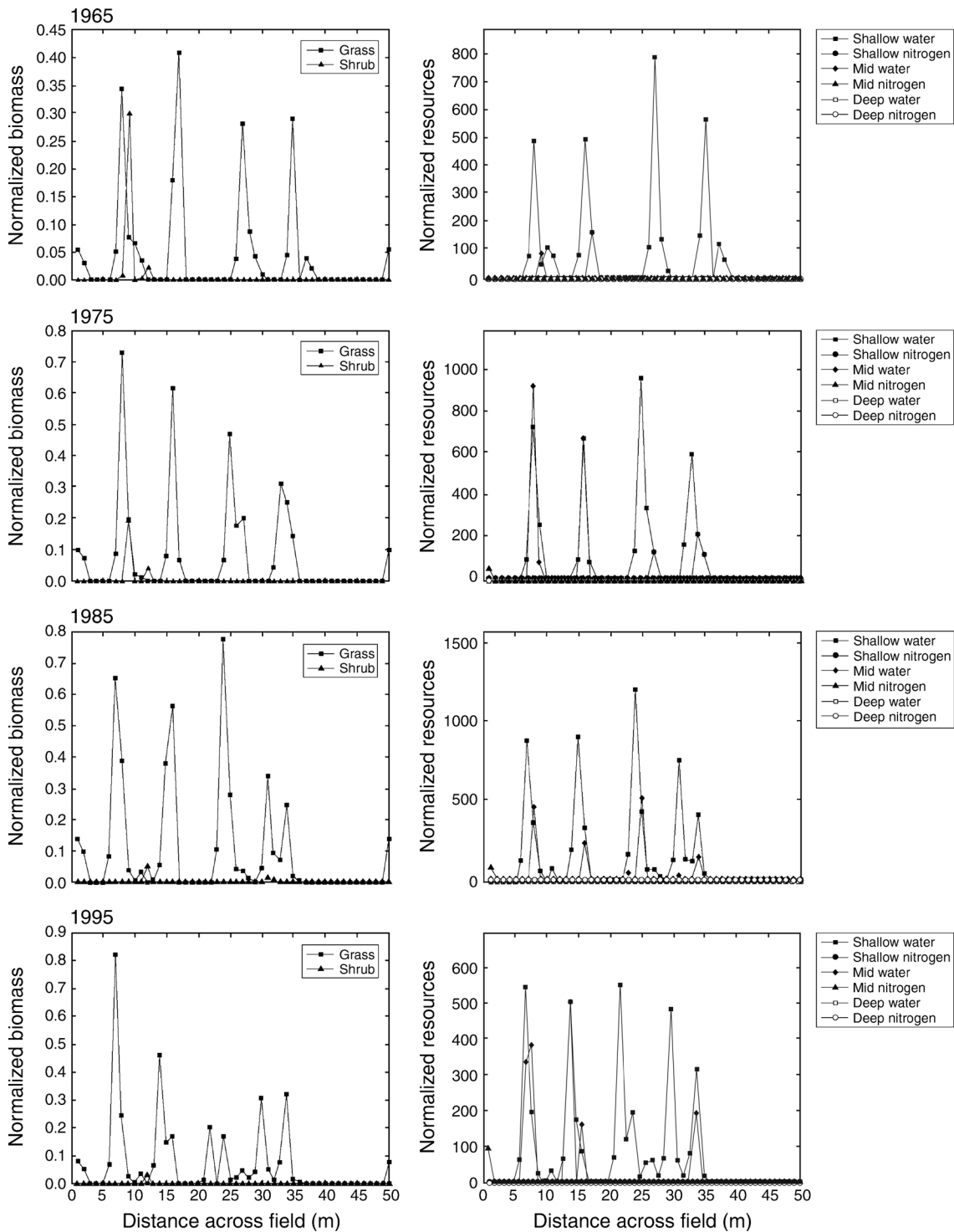


FIG. 17. Continued.

designed to explore causes of spatial complexity as well as predict specific responses to a variety of endogenous and exogenous disturbances. This contribution differs from previous work in that it rests on a sound process-

based understanding and data that has both a clear physical meaning and can be measured in the field. Both abiotic and biotic processes have been considered in greater detail than previous modelling studies, while

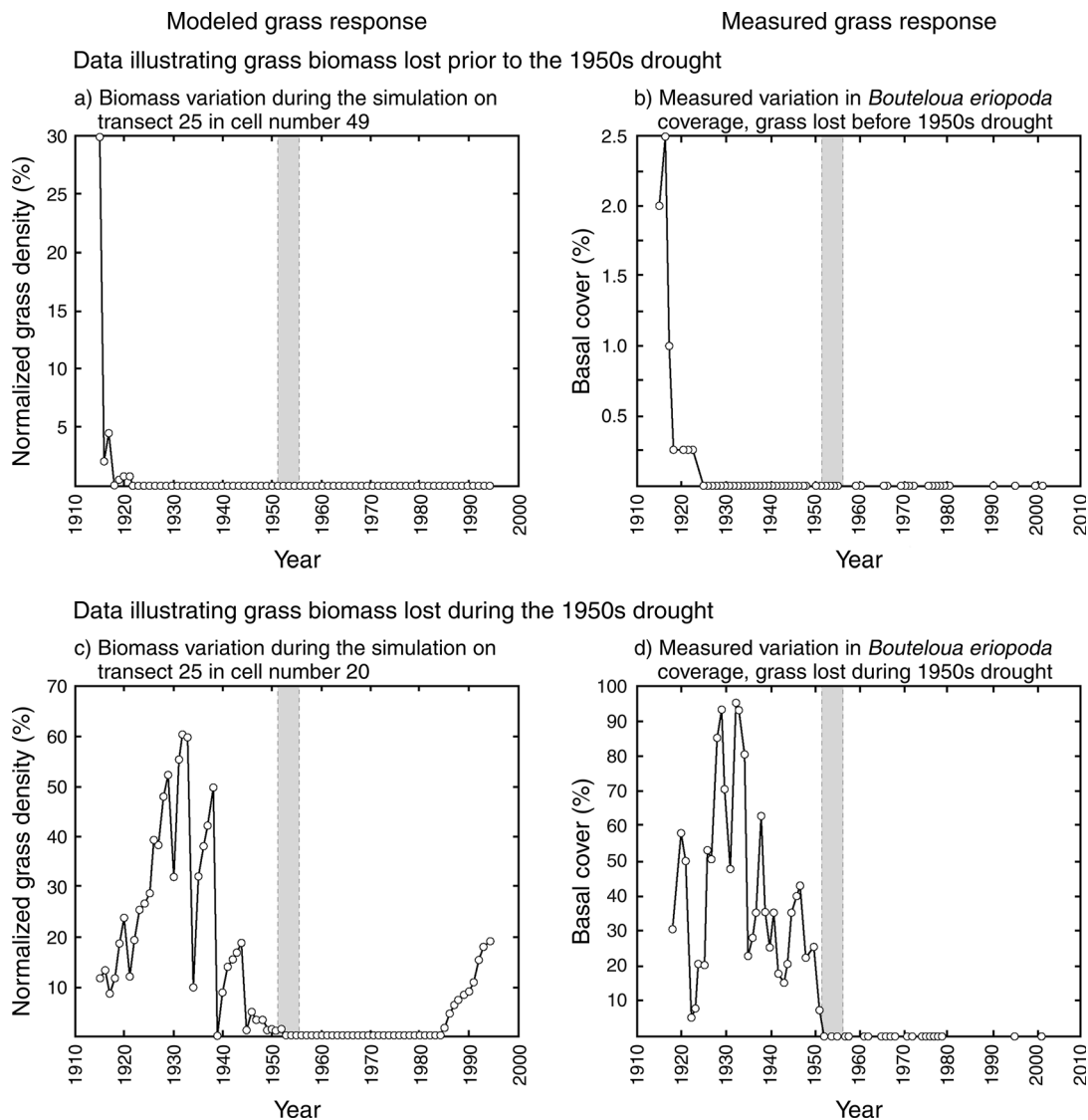


FIG. 18. Selected comparisons of individual cells taken from the center line of the grid compared with experimental-plot data from Yao et al (2006). For ease of representation, modeled biomass is presented as a proportion (normalized biomass) of the maximum potential biomass given in Peters (2002a). The gray-shaded area shows the 1950s drought.

maintaining a level of parsimony that means that parameter uncertainty is unlikely to drown out the effects of the processes under investigation.

A general modelling framework has been developed, and specific implementation of this model was employed to evaluate the framework against data that has been obtained from field studies. In doing so, it is noted that even with the simplifications made, the model was able to closely match measured conditions at the field site, in terms of species response and the generation of plausible patterns of vegetation loss. On this basis, the general framework can be considered to have captured the key processes within the ecosystem and may make a useful contribution toward understanding desert vegetation more straightforwardly.

Rather than developing predictions of vegetation change under hypothetical future scenarios, historical data have been used to retrodict grassland responses to climatic conditions. In doing so, it was possible to compare the model results to current conditions, which comparison provides a robust test of both the model and our understanding of how desert ecosystems operate. Moreover, the approach has led to the generation of a number of testable predictions that can be compared to other field data.

The results suggest that the desert grasslands have been stable under historic conditions for three reasons. First, the structure of the rainfall itself inhibits shrub invasion; secondly, the faster growth rate tends to allow grass to outcompete with shrubs for available resources;

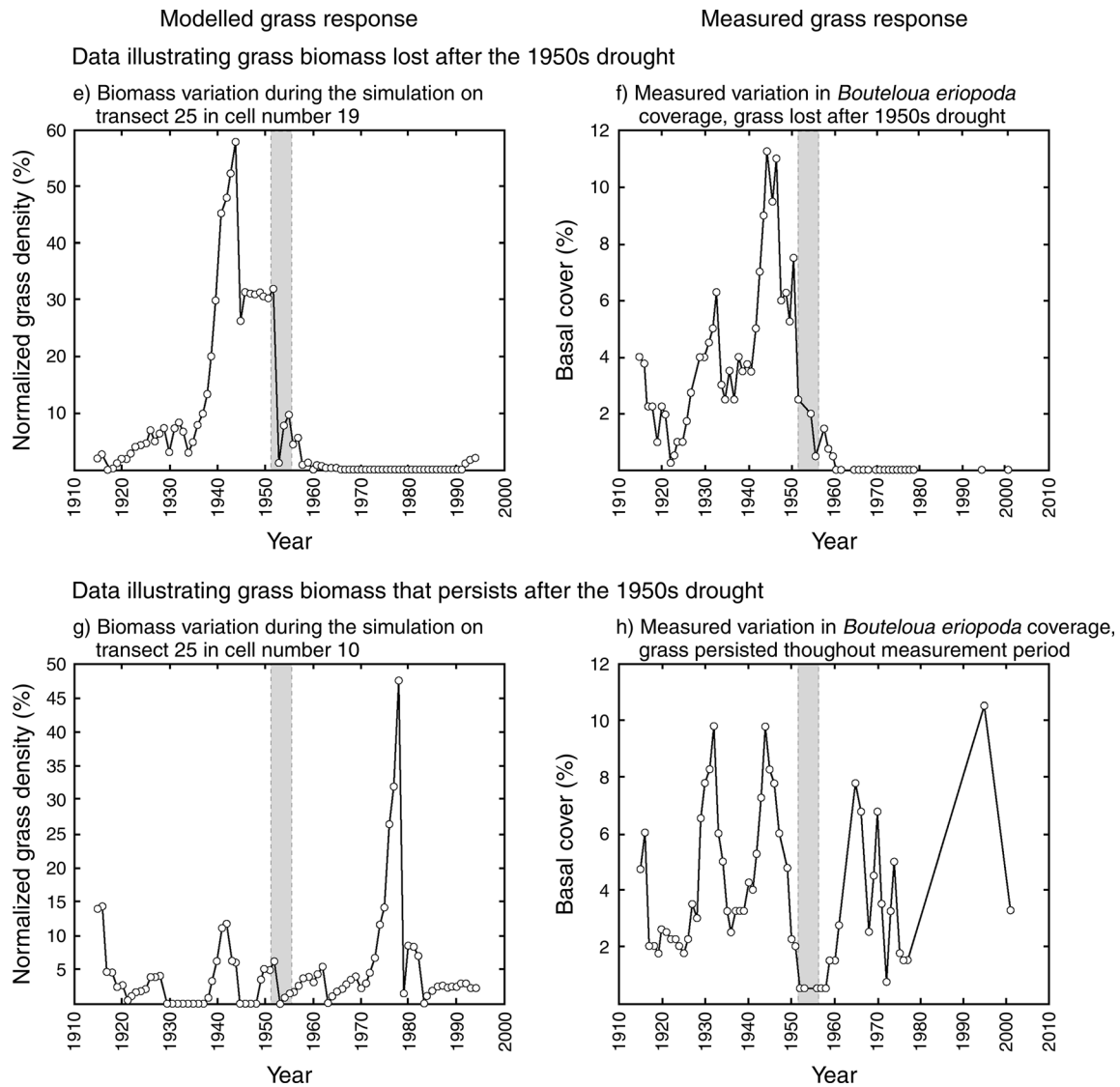


FIG. 18. Continued.

and thirdly, the banding patterns themselves are much more stable structures in semiarid ecosystems than a homogenous distribution of grass. During droughts, the resource that is input to connected cells will flow onto the bands where it supports the patch biomass, and the length of the connected cells and the length of grass bands are related. The resource distribution across patches remains predominantly lateral, with little (or no) resource accumulated beneath the bands. The shrubs (in this simulation) are only able to invade grass stands when a disturbance causes a grass plant to be removed from a location where resource has accumulated, but the persistence of the shrub is also a function of two types of connectivity. First, the length of the connected pathways to the shrub must be longer than the connected pathways to the grass plant, and secondly, shrubs will only survive in locations where they are able

to develop a pronounced vertical distribution of resources beneath them. This difference would suggest that lateral accumulations of resource around a shrub indicate that recent climate conditions have caused a great degree of R and P movement along newly emerged connected pathways, but the absence of that accumulation points toward vector operation along more stable connected pathways. The results point to the introduction of cattle grazing, and specifically overgrazing, as the cause of the historical shrub invasion.

The agreement of the model results with experimental studies indicates that this method has merit and is worth pursuing further. It is acknowledged that the implementation presented here far from perfect in two significant respects. First, we have, for instance, used a number of linear relationships, which would not be appropriate in a more general implementation, and many of the surro-

gate data used here (with respect to the relationships between vectors and resource movement) ought to be parameterized more fully. In particular, experimental data aiming to quantify the redistribution of laterally transported resources at the end of a connected pathway (i.e., Eq. 6) is deserving of attention. The lack of detail supported by field research in these factors means that while we can see that the connected pathways must be longer to enable shrubs to survive than for grass plants, we are not able to quantify them with any confidence. Second, some of our model results are unrealistic. For example, the accumulation of nitrogen in the mid and deep soil layers is unrealistic. As was pointed out in the model parameterization (*Model implementation: Model parameterization: Resources and propagules*), there is a dearth of suitable data for this parameterization. Our results suggest that this dearth of data is a significant limitation on our current understanding. The application of the model to a very specific implementation was worthwhile in order to establish that the general framework produces plausible results, and to inform future experimental work that may obtain data in the form required to establish the causal factors that lead to ecosystem changes. On the basis of this work, vertical and lateral connectivity are key emergent properties of the system, which both control its behavior and provide indicators of its state. If these predictions are shown to be compatible with actual conditions, the model presented here will provide a more certain approach toward preventing further semiarid grassland degradation.

ACKNOWLEDGMENTS

This research was supported by the University of Sheffield and LTER Grant DEB-0618210.

LITERATURE CITED

- Abrahams, A. D., and A. J. Parsons. 1991. Relation between infiltration and stone cover on a semiarid hillslope, southern Arizona. *Journal of Hydrology* 122:49–59.
- Abrahams, A. D., A. J. Parsons, and J. Wainwright. 1995. Effects of vegetation change on interrill runoff and erosion, Walnut Gulch, southern Arizona. *Geomorphology* 13(1–4): 37–48.
- Abrahams, A. D., A. J. Parsons, and J. Wainwright. 2003. Disposition of rainwater under creosotebush. *Hydrological Processes* 17:2555–2566.
- Ackerman, T. L., and S. A. Bamberg. 1974. Phenological studies in the Mojave Desert at Rock Valley. Pages 215–226 in H. Lieth, editor. *Ecological studies: analysis and synthesis*. Springer-Verlag, New York, New York, USA.
- Aguiar, M. R., and O. E. Sala. 1999. Patch structure, dynamics and implications for the functioning of arid ecosystems. *Trends in Ecology and Evolution* 14:273–277.
- Allred, K. W. 1996. *New Mexico's natural heritage: biological diversity in the land of enchantment*. New Mexico Academy of Science, Albuquerque, New Mexico, USA.
- Archer, S., D. S. Schimel, and E. A. Holland. 1995. Mechanisms of shrubland expansion: land use, climate or CO₂. *Climatic Change* 29:91–99.
- Baez, S., J. Fargione, D. I. Moore, S. L. Collins, and J. R. Gosz. 2007. Atmospheric nitrogen deposition in the northern Chihuahuan desert: temporal trends and potential consequences. *Journal of Arid Environments* 68:640–651.
- Bainbridge, D. A., and R. A. Virginia. 1990. Restoration in the Sonoran Desert of California. *Restoration and Management Notes* 8:3–14.
- Barbier, N., P. Couteron, J. Lejoly, V. Deblauwe, and O. Lejeune. 2006. Self-organized vegetation patterning as a fingerprint of climate and human impact on semi-arid ecosystems. *Journal of Ecology* 94:537–547.
- Barbour, M. G. 1969. Age and space distribution of the desert shrub *Larrea divaricata*. *Ecology* 50:679–685.
- Bartley, R., C. H. Roth, J. A. Ludwig, D. McJannet, A. C. Leidloff, J. Corfield, A. Hawdon, and B. Abbot. 2006. Runoff and erosion from Australia's tropical semi-arid rangelands: Influences of ground cover for differing space and time scales. *Hydrological Processes* 20:3317–3333.
- Bracken, L. J., and J. Croke. 2007. The concept of hydrological connectivity and its contribution to understanding runoff-dominated geomorphic systems. *Hydrological Processes* 21:1749–1763.
- Brazier, R. E., A. J. Parsons, J. Wainwright, D. M. Powell, and W. H. Schlesinger. 2007. Upscaling understanding of nitrogen dynamics associated with overland flow in a semi-arid environment. *Biogeochemistry* 82:265–278.
- Brisson, J., and J. F. Reynolds. 1994. The effect of neighbors on root distribution in a creosotebush (*Larrea tridentata*) population. *Ecology* 75:1693–1702.
- Bromley, J., J. Brouwer, A. P. Barker, S. R. Gaze, and C. Valentin. 1997. The role of surface water distribution in an area of patterned vegetation in a semi-arid environment, south west Niger. *Journal of Hydrology* 198:1–29.
- Brown, D. E. 1982. Semi-desert grassland. Biotic communities of the American Southwest—United States and Mexico. *Desert Plants* 4(1–4):123–131.
- Brown, D. W., and P. J. Gersmehl. 1985. Migration models for grasses in the American midcontinent. *Annals of the Association of American Geographers* 75:383–394.
- Buffington, L. C., and C. H. Herbel. 1965. Vegetational changes on a semi-desert grassland range from 1858 to 1963. *Ecological Monographs* 35:139–164.
- Bugmann, H. K. M., and A. M. Solomon. 1995. The use of a European forest model in North America: a study of ecosystem response to climate gradients. *Journal of Biogeography* 22:477–484.
- Burgess, T. L. 1995. Desert grassland, mixed shrub savanna, shrub steppe or semidesert scrub The dilemma of coexisting forms. Pages 31–67 in M. P. McClaran and T. R. Van Devender, editors. *The desert grassland*. University of Arizona Press, Tuscon, Arizona, USA.
- Burke, I. C., D. S. Schimml, C. M. Yonker, W. J. Parton, L. A. Joyce, and W. K. Lauenroth. 1990. Regional modelling of grassland biogeochemistry using GIS. *Landscape Ecology* 4:45–54.
- Campbell, R. S. 1931. Plant succession and grazing capacity on clay soils in southern New Mexico. *Journal of Agricultural Research* 43(12):1027–1051.
- Canfield, R. H. 1948. Perennial grass composition as an indicator of condition of Southwestern mixed grass ranges. *Ecology* 29:190–204.
- Casenave, A., and C. Valentin. 1992. A runoff capability classification-system based on surface-features criteria in semiarid areas of West Africa. *Journal of Hydrology* 130:231–249.
- Casper, B. B., and R. B. Jackson. 1997. Plant competition below ground. *Annual Review of Ecological Systems* 28:545–570.
- Castellanos, A. E., and F. E. Molina. 1990. Differential survivorship and establishment in *Simmondsia chinensis* (jajoba). *Journal of Arid Environments* 19:65–76.
- Castets, V., E. Dulos, J. Boissonade, and P. De Kepper. 1990. Experimental evidence of a sustained standing Turing-type nonequilibrium chemical pattern. *Physical Review Letters* 64:2953–2956.

- Chandrasekhar, S., editor. 1961. Hydrodynamic and hydro-magnetic stability. Springer-Verlag, Berlin, Germany.
- Charley, J. L., and N. E. West. 1975. Plant-induced soil chemical patterns in some shrub-dominated semi-desert ecosystems of Utah. *Journal of Ecology* 63:945–963.
- Chew, R., and A. E. Chew. 1970. Energy relationships of the mammals of a desert shrub (*Larrea tridentata*) community. *Ecological Monographs* 40:1–21.
- Clark, C. M., and D. Tilman. 2008. Loss of plant species after chronic low-level nitrogen deposition to prairie grasslands. *Nature* 451:712–715.
- Clos-Arceuduc, M. 1956. Etude sur photographies aeriennes d'une formation vegetale sahelienne: la brousse tigree. *Bulletin de l'IFAN Serie A* 18:678–684.
- Cody, M. L. 1986. Spacing patterns in the Mojave Desert plant communities: near neighbour analysis. *Journal of Arid Environments* 11:199–217.
- Coffin, D. P., and W. K. Lauenroth. 1990. A gap dynamics simulation model of succession in the shortgrass steppe. *Ecological Modeling* 49:229–266.
- Comrie, A. C., and B. Broyles. 2002. Variability and spatial modelling of fine-scale precipitation data for the Sonoran Desert of south-west Arizona. *Journal of Arid Environments* 50:573–592.
- Cornet, A., J. P. Delahoume, and C. Montana, editors. 1988. Dynamics of striped vegetation patterns and water balance in the Chihuahuan Desert. SBP Academic Publishing, The Hague, The Netherlands.
- Couteron, P., and O. Lejeune. 2001. Periodic spotted patterns in semi-arid vegetation explained by a propagation-inhibition model. *Journal of Ecology* 89:616–628.
- Dakos, V., S. Kéfi, M. Rietkerk, E. M. van Nes, and M. Scheffer. 2011. Slowing down in spatially patterned ecosystems at the brink of collapse. *American Naturalist* 177:E153–E166.
- d'Arigo, R. D., and G. C. Jacoby. 1992. A tree-ring reconstruction of New Mexico winter precipitation and its relation to El Niño/Southern Oscillation events. Pages 7–28 in H. F. Diaz and V. Markgraf, editors. *El Niño. Historical and paleoclimatic aspects of the Southern Oscillation*. Cambridge University Press, Cambridge, UK.
- Deblauwe, V., N. Barbier, P. Couteron, O. Lejeune, and J. Bogaert. 2008. The global biogeography of semi-arid periodic vegetation patterns. *Global Ecology and Biogeography* 17:715–723.
- d'Herbes, J. M., C. Valentin, and D. J. Tongway, editors. 2001. Banded vegetation patterning in arid and semiarid environments; ecological processes and consequences for management. Springer, Heidelberg, Germany.
- D'Odorico, P., F. Laio, and L. Ridolfi. 2006. Patterns as indicators of productivity enhancement by facilitation and competition in dryland vegetation. *Journal of Geophysical Research* 111:G03010.
- Dunkerley, D. L., and K. J. Brown. 1999. Banded vegetation near Broken Hill, Australia: significance of surface roughness and soil physical properties. *Catena* 37(1–2):75–88.
- Fitter, A. H., and R. K. M. Hay. 1987. Environmental physiology of plants. Second edition. Academic Press, London, UK.
- Furukawa, K., K. Imai, and M. Kurashige. 2000. Simulated effect of box size and wall on porosity of random packings of spherical particles. *Acta Mechanica* 140:219–231.
- Gallardo, A., and W. H. Schlesinger. 1992. Carbon and nitrogen limitations of soil microbial biomass in desert ecosystems. *Biogeochemistry* 18:1–17.
- Gardener, J. L. 1950. The effects of thirty years of protection from grazing in desert grasslands. *Ecology* 31:44–50.
- Gibbens, R. P., and J. M. Lenz. 2001. Root system of some Chihuahuan Desert plants. *Journal of Arid Environments* 49:221–263.
- Gibbens, R. P., R. P. McNeely, K. M. Havstad, R. F. Beck, and B. Nolen. 2005. Vegetation changes in the Jornada Basin from 1858 to 1998. *Journal of Arid Environments* 61:651–668.
- Gillett, J. 1941. The plant formations of western British Somaliland and the Harar province of Abyssinia. *Kew Bulletin* 2:37–75.
- Goldberg, D. E., and R. M. Turner. 1986. Vegetation change and plant demography in permanent plots in the Sonoran desert. *Ecology* 67:695–712.
- Gosz, R. J., and J. R. Gosz. 1996. Species interactions on the biome transition zone in New Mexico: response of blue grama (*Bouteloua gracilis*) and black grama (*Bouteloua eriopoda*) to fire and herbivory. *Journal of Arid Environments* 34:101–114.
- Greene, R. S. B., P. I. A. Kinnell, and J. T. Wood. 1994. Role of plant cover and stock trampling on runoff and soil erosion from semi-arid wooded rangelands. *Australian Journal of Soil Research* 32:954–973.
- Greig-Smith, P. 1979. Pattern in vegetation. *Journal of Ecology* 67:755–779.
- Grimm, V., and S. F. Railsback. 2005. Individual-based modelling and ecology. Princeton University Press, Princeton, New Jersey, USA.
- Havstad, K. M., L. F. Huenneke, and W. H. Schlesinger, editors. 2006. Structure and function of a Chihuahuan Desert ecosystem: the Jornada Basin Long-Term Ecological Research Site. Oxford University Press, New York, New York, USA.
- Herbel, C. H., F. N. Ares, and R. A. Wright. 1972. Drought effects on a semidesert grassland range. *Ecology* 53:1084–1093.
- Higgins, S. I., D. M. Richardson, and R. M. Cowling. 1996. Modeling invasive plant spread: the role of plant-environment interactions and model structure. *Ecology* 77:2043–2054.
- Hillel, D. 2004. Introduction to soil physics. Elsevier, Amsterdam, The Netherlands.
- HilleRisLambers, R., M. Rietkerk, F. van den Bosch, H. H. T. Prins, and H. de Croon. 2001. Vegetation Pattern formation in semiarid grazing systems. *Ecology* 82:50–61.
- Hooper, D. U., and L. Johnson. 1999. Nitrogen limitation in dryland ecosystems: responses to geographical and temporal variation in precipitation. *Biogeochemistry* 46:247–293.
- Humphrey, R. R. 1958. The desert grassland: a history of vegetational change and an analysis of causes. *Botanical Review* 24:164–193.
- Humphrey, R. R., and L. A. Mehrhoff. 1958. Vegetation changes on a southern Arizona grassland range. *Ecology* 39:720–726.
- Istanbulluoglu, E., and R. L. Bras. 2006. On the dynamics of soil moisture, vegetation, and erosion: Implications of climate variability and change. *Water Resources Research* 42: W06418.
- Kéfi, S., M. Rietkerk, M. van Baalen, and M. Loreau. 2007. Local facilitation, bistability and transitions in arid ecosystems. *Theoretical Population Biology* 71:367–379.
- Klausmeier, C. A. 1999. Regular and irregular patterns in semiarid vegetation. *Science* 284:1826–1828.
- Kot, M. 2001. Elements of mathematical ecology. Cambridge University Press, Cambridge, UK.
- Lange, R. T., A. D. Nicholson, and D. A. Nicholson. 1984. Vegetation management of chenopod rangelands in South Australia. *Australian Rangeland Journal* 6:46–54.
- Leach, A. R. 2001. Molecular modelling: principals and applications. Prentice Hall, Englewood Cliffs, New Jersey, USA.
- Lefever, R., N. Barbier, P. Couteron, and O. Lejeune. 2009. Deeply gapped vegetation patterns: on crown/root allometry, criticality and desertification. *Journal of Theoretical Biology* 261:194–209.

- Li, J., G. S. Okin, L. J. Hartman, and H. E. Epstein. 2007. Quantitative assessment of wind erosion and soil nutrient loss in desert grasslands of southern New Mexico, USA. *Biogeochemistry* 85:317–332.
- Loreau, M., S. Naeem, and P. Inchausti. 2002. Biodiversity and ecosystem functioning: synthesis and perspectives. Oxford University Press, Oxford, UK.
- Ludwig, J. A., B. P. Wilcox, D. D. Breshears, D. J. Tongway, and A. C. Imeson. 2005. Vegetation patches and runoff-erosion as interacting ecohydrological processes in semiarid landscapes. *Ecology* 86:288–297.
- MacFadyan, W. A. 1950. Vegetation patterns in the semi-desert plains of British Somaliland. *Geographical Journal* 116:199–210.
- Maneta, M. P., S. Schnabel, W. W. Wallender, S. Panday, and V. Jetten. 2008. Calibration of an evapotranspiration model to simulate soil water dynamics in a semiarid rangeland. *Hydrological Proceedings* 22:4655–4669.
- Martinez-Meza, E., and W. G. Whitford. 1996. Stemflow, throughfall and channelization of stemflow by roots in three Chihuahuan desert shrubs. *Journal of Arid Environments* 32:271–287.
- Mauchamp, A., C. Montana, J. Lepart, and S. Rambal. 1993. Ecotone dependent recruitment of a desert shrub, *Flourensia cernua*, in vegetation stripes. *Oikos* 68:107–116.
- May, R. M. 1977. Thresholds and breakpoints in ecosystems with a multiplicity of stable states. *Nature* 269–477.
- McAuliffe, J. R. 1988. Markovian dynamics of simple and complex desert plant communities. *American Naturalist* 131:459–490.
- McClaran, M. P., and T. R. Van Devender. 1995. The desert grassland. Tucson University of Arizona Press, Tucson, Arizona, USA.
- McPherson, G. R., H. A. Wright, and D. B. Wester. 1988. Patterns of shrub invasion in semi-arid Texas grasslands. *American Midland Naturalist* 120:391–397.
- Meinhardt, H. 1982. Models of biological patterns formation. Academic, New York, New York, USA.
- Michaelides, K., D. Lister, J. Wainwright, and A. J. Parsons. 2012. Linking runoff and erosion dynamics to nutrient fluxes in a degrading dryland landscape. *Journal of Geophysical Research—Biogeosciences* 117:G00N15.
- Miller, R. F., and G. B. Donart. 1979. Response of *Bouteloua eriopoda* Torr. and *Sporobolus flexuosus* (Thurb.) Rhbd. to season of defoliation. *Journal of Range Management* 32:449–452.
- Monger, H. C., and B. T. Bestelmeyer. 2006. The soil-geomorphic template and biotic change in arid and semi-arid ecosystems. *Journal of Arid Environments* 65:207–218.
- Montana, C. 1992. The colonization of bare areas in two phase mosaics of an arid ecosystem. *Journal of Ecology* 80:315–327.
- Morgan, R. P. C. 1996. Soil erosion and conservation. Second edition. Longman, Harlow, UK.
- Müller, E. N., J. Wainwright, and A. J. Parsons. 2007. The impact of connectivity on the modelling of water fluxes in semi-arid shrubland environments. *Water Resources Research* 43. <http://dx.doi.org/10.1029/2006WR005006>
- Müller, E. N., J. Wainwright, and A. J. Parsons. 2008. Spatial variability of soil and nutrient parameters within grasslands and shrublands of a semi-arid environment, Jornada Basin, New Mexico. *Ecohydrology* 1:3–12.
- Murray, J. D. 1989. Mathematical biology. Springer-Verlag, Berlin, Germany.
- Nash, M. S., E. Jackson, and W. G. Whitford. 2004. Effects of intense, short-duration grazing on micro-topography in a Chihuahuan Desert grassland. *Journal of Arid Environments* 56(3):383–393.
- Neilson, R. P. 1986. High-resolution climatic analysis and Southwest biogeography. *Science* 232:27–34.
- Nelson, E. W. 1934. The influence of precipitation and grazing upon black grama grass range. U.S. Department of Agriculture, Washington, D.C., USA.
- Nicholson, S. E. 1979. Revised rainfall series for the West African subtropics. *Monthly Weather Review* 107:620–623.
- Nicholson, S. E. 1981. Rainfall and atmospheric circulation during drought periods and wetter years in West Africa. *Monthly Weather Review* 109:2191–2208.
- Nicolis, G., and I. Prigogine. 1977. Self-organization in non-equilibrium systems. John Wiley and Sons, New York, New York, USA.
- Noy-Meir, I. 1973. Desert ecosystems: environment and producers. *Annual Review of Ecology* 4:25–51.
- Okin, G. S., P. D. D’Odorico, and S. Archer. 2009. Impact of feedbacks on Chihuahuan desert grasslands: transience and metastability driven by grass recruitment. *Journal of Geophysical Research—Biogeosciences* 114:G01004.
- Okin, G. S., and D. A. Gillette. 2001. Distribution of vegetation in wind-dominated landscapes: Implications for wind erosion modelling and landscape processes. *Journal of Geophysical Research* 106:9673–9683.
- Okin, G. S., J. E. Herrick, and D. A. Gillette. 2006. Multiscale controls on and consequences of aeolian processes in landscape change in arid and semiarid environments. *Journal of Arid Environments* 65:253–275.
- Okin, G. S., B. Murray, and W. H. Schlesinger. 2001. Degradation of sandy arid shrubland environments: observations, process modelling and management implications. *Journal of Arid Environments* 47:123–144.
- Okin, G. S., A. J. Parsons, J. Wainwright, J. E. Herrick, B. T. Bestelmeyer, D. P. C. Peters, and E. L. Fredrickson. 2009. Do changes in connectivity explain desertification? *BioScience* 59:237–244.
- Osborne, C. P., and D. J. Beerling. 2006. Nature’s green revolution: the remarkable evolutionary rise of C₄ plants. *Philosophical Transactions of the Royal Society B* 361:173–194.
- Parshall, T., D. R. Foster, E. Faison, D. MacDonald, and B. C. S. Hansen. 2003. Long-term history of vegetation and fire in pitch pine-oak forests on Cape Cod, Massachusetts. *Ecology* 84:736–748.
- Parsons, A. J., A. D. Abrahams, and S. H. Luk. 2006a. Size characteristics of sediment in interrill overland flow on a semiarid hillslope, Southern Arizona. *Earth Surface Processes and Landforms* 16:143–152.
- Parsons, A. J., A. D. Abrahams, and J. R. Simanton. 1992. Microtopography and soil-surface materials on semi-arid piedmont hillslopes, southern Arizona. *Journal of Arid Environments* 22:107–115.
- Parsons, A. J., A. D. Abrahams, and J. Wainwright. 1996. Responses of interrill runoff and erosion rates to vegetation change in southern Arizona. *Geomorphology* 14:311–317.
- Parsons, A. J., R. E. Brazier, J. Wainwright, and D. Powell. 2006b. Scale relations in hillslope runoff and erosion. *Earth Surface Processes and Landforms* 31:1384–1393.
- Parsons, A. J., J. Wainwright, A. D. Abrahams, and J. R. Simanton. 1997. Distributed dynamic modelling of interrill overland flow. *Hydrological Processes* 11:1833–1859.
- Parsons, A. J., J. Wainwright, D. M. Powell, J. Kaduk, and R. Brazier. 2004. A conceptual model for determining soil erosion by water. *Earth Surface Processes and Landforms* 29:1293–1302.
- Parton, W. J. 1978. Dynamics of C, N, P and S in grassland soils: a model. *Biogeochemistry* 5:109–131.
- Paulsen, H. A., Jr., and F. N. Ares. 1962. Grazing values and management of black grama and tobosa grasslands and associated shrub ranges of the Southwest. Technical Bulletin No. 1270. U.S. Department of Agriculture, Forest Service, Washington, D.C., USA.
- Peters, D. P. C. 2002a. Plant species dominance at a grassland-shrubland ecotone: an individual-based gap dynamics model

- of herbaceous and woody species. *Ecological Modelling* 152:5–32.
- Peters, D. P. C. 2002*b*. Recruitment potential of two perennial grasses with different growth forms at a semiarid-arid transition zone. *American Journal of Botany* 89(10):1616–1623.
- Peters, D. P. C., B. T. Bestelmeyer, J. E. Herrick, E. Fredrickson, H. C. Monger, and K. M. Havstad. 2006*a*. Disentangling complex landscapes: new insights to forecasting arid and semiarid system dynamics. *BioScience* 56:491–501.
- Peters, D. P. C., J. R. Gosz, W. T. Pockman, E. E. Small, R. Parmenter, S. L. Collins, and E. Muldavin. 2006*b*. Integrating patch and boundary dynamics to understand and predict biotic transitions at multiple scales. *Landscape Ecology* 21:19–23.
- Peters, D. P. C., J. R. Gosz, W. T. Pockman, E. E. Small, R. Parmenter, S. L. Collins, E. Polley, H. B. Johnson, and J. D. Derner. 2002. Soil- and plant-water dynamics in a C3/C4 grassland exposed to a subambient to superambient CO₂ gradient. *Global Change Biology* 8:1118–1129.
- Pockman, W. T., and J. S. Sperry. 1997. Freezing-induced xylem cavitation and the northern limit of *Larrea tridentata*. *Oecologia* 109:19–27.
- Rango, A., M. Chopping, J. Ritchie, K. Havstad, W. Kustas, and T. Schmugge. 2000. Morphological characteristics of shrub coppice dunes in desert grasslands of southern New Mexico derived from scanning LIDAR. *Remote Sensing of Environment* 74:26–44.
- Reynolds, J. F., R. A. Virginia, P. R. Kemp, A. G. de Souza, and D. C. Tremmel. 1999. Impact of drought on desert shrubs: effects of seasonality and degree of resource island development. *Ecological Monographs* 69:69–106.
- Rietkerk, M., M. C. Boerlijrs, F. van Langevelde, R. HilleRisLambers, J. Van de Koppel, L. Kumar, and A. M. de Roos. 2002. Self-organization of vegetation in arid ecosystems. *American Naturalist* 160:524–530.
- Rietkerk, M. F., and J. Van der Koppel. 1997. Alternate stable states and threshold effects in semi-arid grazing systems. *Oikos* 79:69–76.
- Romney, E. M., A. Wallace, and B. Hunter. 1989. Pulse establishment of woody shrubs of denuded Mojave Desert land. Pages 54–57 in A. Wallace, E. D. McArthur, and M. R. Haferkamp, editors. Symposium on shrub ecophysiology and biotechnology. U.S. Department of Agriculture, Forest Service, Intermountain Research station, Logan, Utah, USA.
- Rovinsky, A. B. 1987. Twinkling patterns and diffusion-induced chaos in a model of the Belousov-Zhabotinsky Chemical Medium. *Journal of Physical Chemistry* 91:4606.
- Schlesinger, W. H., and W. T. Peterjohn. 1991. Processes controlling ammonia volatilization from Chihuahuan desert soils. *Soil Biology and Biochemistry* 23:637–642.
- Schlesinger, W. H., and A. M. Pilmanis. 1998. Plant-soil interactions in deserts. *Biogeochemistry* 42:169–187.
- Schlesinger, W. H., J. A. Raikes, A. E. Hartley, and A. F. Cross. 1996. On the spatial pattern of soil nutrients in desert ecosystems. *Ecology* 77:364–374.
- Schlesinger, W. H., J. F. Reynolds, G. L. Cunningham, L. F. Huenneke, W. M. Jarrell, R. A. Virginia, and W. G. Whitford. 1990. Biological feedbacks in global desertification. *Science* 247:1043–1048.
- Scoging, H. 1992. Modelling overland-flow hydrology for dynamic hydraulics. Pages 89–103 in Overland flow hydraulics and erosion mechanics. A. J. Parsons and A. D. Abrahams, editors. UCL Press, London, UK.
- Scott, R. L., W. L. Cable, and K. R. Hultine. 2008. The ecohydrological significance of hydraulic redistribution in a semiarid savanna. *Water Resources Research* 44:W02440.
- Seghier, J., S. Galle, J. L. Rajot, and M. Ehrmann. 1997. Relationships between soil moisture and growth of herbaceous plants in a natural vegetation mosaic in Niger. *Journal of Arid Environments* 36:87–102.
- Slatyer, R. O. 1961. Methodology of a water balance study conducted on a desert woodland (*Acacia anuera* F. Muell) community in central Australia. UNESCO Arid Zone Research 16:15–26.
- Smith, G., J. L. Holechek, and M. Cardenas. 1996. Wildlife numbers on excellent and good condition Chihuahuan Desert rangelands: an observation. *Journal of Range Management* 49:489–493.
- Starfield, A. M. 1996. Model of transient changes in arctic and boreal vegetation in response to climate and land use change. *Ecological Applications* 6:842–864.
- Sun, G., D. P. Coffin, and W. K. Lauenroth. 1998. Comparison of root distributions of species of North American grasslands using GIS. *Journal of Vegetation Science* 8:587–596.
- Taylor, P. D., L. Fahrig, K. Henein, and G. Merriam. 1993. Connectivity is a vital element of landscape structure. *Oikos* 68:571–573.
- Thornes, J. B. 1990. The interaction of erosional and vegetational dynamics in land degradation: spatial outcomes. Pages 41–53 in J. B. Thornes, editor. *Vegetation and erosion*. John Wiley and Sons, Chichester, UK.
- Thornes, J. B. 2007. Modelling soil erosion by grazing: recent developments and new approaches. *Geographical Research* 45:13–26.
- Thornes, J. B., and J. Brandt. 1993. Erosion-vegetation competition in a stochastic environment undergoing climatic change. Pages 306–320 in A. C. Millington and K. J. Pye, editors. *Environmental change in the drylands: biogeographical and geomorphological responses*. John Wiley and Sons, Chichester, UK.
- Tongway, D. J., and J. A. Ludwig, editors. 2001. *Theories on the origins, maintenance, dynamics and functioning of banded landscapes*. Springer, Heidelberg, Germany.
- Turchin, P. 2003. *Complex population dynamics*. Princeton University Press, Princeton, New Jersey, USA.
- Turing, A. M. 1952. The chemical basis of morphogenesis. *Philosophical Transactions of the Royal Society B* 237:37–72.
- Turnbull, L., J. Wainwright, and R. E. Brazier. 2008. A conceptual framework for understanding semi-arid land degradation: ecohydrological interactions across multiple-space and time scales. *Ecohydrology* 1:23–34.
- Turnbull, L., J. Wainwright, and R. E. Brazier. 2010. Nitrogen and phosphorus dynamics during runoff events over a transition from grassland to shrubland in the south-western United States. *Hydrological Processes* 24:393–414.
- Turner, M. G., W. H. Romme, R. H. Gardner, R. V. O'Neill, and T. K. Kratz. 1993. A revised concept of landscape equilibrium: disturbance and stability on scaled landscapes. *Landscape Ecology* 8:213–227.
- van de Koppel, J., and M. Rietkerk. 2004. Spatial interactions and resilience in arid ecosystems. *American Naturalist* 163:113–121.
- Versteeg, H. K., and W. Malalasekera. 1995. *An introduction to computational fluid dynamics: the finite volume method*. Prentice Hall, London, UK.
- Wainwright, J. 2005. Climate and climatological variations in the Jornada Experimental Range and neighbouring areas of the US Southwest. *Advances in Environmental Monitoring and Modeling* 1:39–110.
- Wainwright, J. 2009. Desert ecogeomorphology. Pages 21–66 in A. J. Parsons and A. D. Abrahams, editors. *Geomorphology of desert environments*. Second edition. Springer, Berlin, Germany.
- Wainwright, J., and L. J. Bracken. 2011. Overland flow and runoff generation. Pages 235–268 in D. S. G. Thomas, editor. *Arid zone geomorphology*. Third edition. John Wiley and Sons, Chichester, UK.

- Wainwright, J., and A. J. Parsons. 2002. The effect of temporal variations in rainfall on scale dependency in runoff coefficients. *Water Resources Research* 38(12):1271.
- Wainwright, J., and A. J. Parsons. 2010. Thornes, J.B. 1985: The ecology of erosion. *Geography* 70:222–35. *Progress in Physical Geography* 34:399–408.
- Wainwright, J., A. J. Parsons, and A. D. Abrahams. 1999. Field and computer simulation experiments on the formation of desert pavement. *Earth Surface Processes and Landforms* 24:1025–1037.
- Wainwright, J., A. J. Parsons, and A. D. Abrahams. 2000. Plot-scale studies of vegetation, overland flow and erosion interactions: case studies from Arizona and New Mexico. *Hydrological Processes* 14:2921–2943.
- Wainwright, J., A. J. Parsons, W. H. Schlesinger, and A. D. Abrahams. 2002. Hydrology–vegetation interactions in areas of discontinuous flow on a semi-arid bajada, southern New Mexico. *Journal of Arid Environments* 51:319–330.
- Wainwright, J. W., A. J. Parsons, E. N. Müller, R. E. Brazier, D. M. Powell, and B. Fenti. 2008a. A transport-distance approach to scaling erosion rates: 1. Background and model development. *Earth Surface Processes and Landforms* 33:813–826.
- Wainwright, J. W., A. J. Parsons, E. N. Müller, R. E. Brazier, D. M. Powell, and B. Fenti. 2008b. A transport-distance approach to scaling erosion rates: 2. Sensitivity and evaluation of MAHLERAN. *Earth Surface Processes and Landforms* 33:962–984.
- Wainwright, J. W., A. J. Parsons, E. N. Müller, R. E. Brazier, D. M. Powell, and B. Fenti. 2008c. A transport-distance approach to scaling erosion rates: 3. Evaluating scaling characteristics of MAHLERAN. *Earth Surface Processes and Landforms* 33:1113–1128.
- Walter, H. 1971. *Ecology of tropical and subtropical vegetation*. Oliver and Boyd, Edinburgh, UK.
- Ward, D. 2008. *The biology of deserts*. Oxford University Press, Oxford, UK.
- Went, F. W., and M. Westergaard. 1949. *Ecology of desert plants*. III. Development of plants in the Death Valley National Monument, California. *Ecology* 30:26–38.
- Western, A. W., G. Bloschl, and R. B. Grayson. 2001. Towards capturing hydrologically significant connectivity in spatial patterns. *Water Resources Research* 37:83–97.
- Westoby, M. 1980. Elements of a theory of vegetation dynamics in arid rangelands. *Israel Journal of Botany* 28:169–194.
- Westoby, M., B. Walker, and I. Noy-Meir. 1989. Opportunistic management for rangelands not at equilibrium. *Journal of Range Management* 42(4):266–274.
- White, L. P. 1997. Vegetation stripes on sheet wash surfaces. *Journal of Ecology* 59:615–622.
- Whitford, W. G. 2002. *Ecology of desert systems*. Academic Press, San Diego, California, USA.
- Williams, C. A., and J. D. Albertson. 2006. Dynamical effects of the statistical structure of annual rainfall on dryland vegetation. *Global Change Biology* 12:777–792.
- Yao, J., D. P. C. Peters, K. M. Havstad, R. P. Gibbens, and J. E. Herrick. 2006. Multi-scale factors and long-term responses of Chihuahuan Desert grasses to drought. *Landscape Ecology* 21:1217–1231.

SUPPLEMENTAL MATERIAL

Appendix

Exploration of model behavior ([Ecological Archives M084-013-A1](#)).